NASA/TM-2021-104606/Vol. 58

Technical Report Series on Global Modeling and Data Assimilation, Volume 58

Randal D. Koster, Editor

Soil Moisture Active Passive (SMAP) Project Assessment Report for Version 5 of the L4_SM Data Product

Rolf H. Reichle, Qing Liu, Randal D. Koster, Joseph V. Ardizzone, Andreas Colliander, Wade T. Crow, Gabrielle J. M. De Lannoy and John S. Kimball

August 2021

NASA STI Program ... in Profile

Since its founding, NASA has been dedicated to the advancement of aeronautics and space science. The NASA scientific and technical information (STI) program plays a key part in helping NASA maintain this important role.

The NASA STI program operates under the auspices of the Agency Chief Information Officer. It collects, organizes, provides for archiving, and disseminates NASA's STI. The NASA STI program provides access to the NTRS Registered and its public interface, the NASA Technical Reports Server, thus providing one of the largest collections of aeronautical and space science STI in the world. Results are published in both non-NASA channels and by NASA in the NASA STI Report Series, which includes the following report types:

- TECHNICAL PUBLICATION. Reports of completed research or a major significant phase of research that present the results of NASA Programs and include extensive data or theoretical analysis. Includes compilations of significant scientific and technical data and information deemed to be of continuing reference value. NASA counterpart of peer-reviewed formal professional papers but has less stringent limitations on manuscript length and extent of graphic presentations.

- TECHNICAL MEMORANDUM. Scientific and technical findings that are preliminary or of specialized interest, e.g., quick release reports, working papers, and bibliographies that contain minimal annotation. Does not contain extensive analysis.

- CONTRACTOR REPORT. Scientific and technical findings by NASA-sponsored contractors and grantees.

- CONFERENCE PUBLICATION. Collected papers from scientific and technical conferences, symposia, seminars, or other meetings sponsored or co-sponsored by NASA.

- SPECIAL PUBLICATION. Scientific, technical, or historical information from NASA programs, projects, and missions, often concerned with subjects having substantial public interest.

- TECHNICAL TRANSLATION. English-language translations of foreign scientific and technical material pertinent to NASA's mission.

Specialized services also include organizing and publishing research results, distributing specialized research announcements and feeds, providing information desk and personal search support, and enabling data exchange services.

For more information about the NASA STI program, see the following:

- Access the NASA STI program home page at http://www.sti.nasa.gov

- E-mail your question to help@sti.nasa.gov

- Phone the NASA STI Information Desk at 757-864-9658

- Write to:
  NASA STI Information Desk
  Mail Stop 148
  NASA Langley Research Center
  Hampton, VA 23681-2199

NASA/TM-2021-104606/Vol. 58

Technical Report Series on Global Modeling and Data Assimilation, Volume 58

Randal D. Koster, Editor

Soil Moisture Active Passive (SMAP) Project Assessment Report for Version 5 of the L4_SM Data Product

Rolf H. Reichle
Global Modeling and Assimilation Office, NASA Goddard Space Flight Center, Greenbelt, MD

Qing Liu
Science Systems and Applications Inc., Lanham, MD

Randal D. Koster
Global Modeling and Assimilation Office, NASA Goddard Space Flight Center, Greenbelt, MD

Joseph V. Ardizzone
Science Systems and Applications Inc., Lanham, MD

Andreas Colliander
Jet Propulsion Laboratory, Caltech, Pasadena, CA

Wade T. Crow
U.S. Department of Agriculture, Agricultural Research Service, Beltsville, MD

Gabrielle J. M. De Lannoy
KULeuven, Leuven, Belgium

John S. Kimball
University of Montana, Missoula, MT

National Aeronautics and
Space Administration

Goddard Space Flight Center
Greenbelt, Maryland 20771

August 2021

Level of Review: This material has been technically reviewed by technical management.

Available from

NASA STI Program
Mail Stop 148
NASA's Langley Research
Center Hampton, VA
23681-2199

National Technical Information
Service 5285 Port Royal Road
Springfield, VA 22161
703-605-6000

TABLE OF CONTENTS

EXECUTIVE SUMMARY

This report provides an assessment of Version 5 of the SMAP Level 4 Surface and Root Zone Soil Moisture (L4_SM) product, which was first released on 27 August 2020. The assessment includes comparisons of L4_SM soil moisture estimates with in situ measurements from SMAP core validation sites and sparse networks. The assessment further provides a global evaluation of the internal diagnostics from the ensemble-based data assimilation system that is used to generate the L4_SM product, including observation-minus-forecast (O-F) brightness temperature residuals and soil moisture analysis increments. Together, the core validation site comparisons and the statistics of the assimilation diagnostics are considered primary validation methodologies for the L4_SM product. Comparisons against in situ measurements from regional-scale sparse networks are considered a secondary validation methodology because such in situ measurements are subject to upscaling errors from the point-scale to the grid-cell scale of the data product.

The Version 5 L4_SM algorithm was recalibrated to work with the substantially changed calibration of the assimilated Version 5 (R17) Level-1C brightness temperatures. Specifically, the brightness temperature scaling parameters in the Version 5 L4_SM algorithm are based on five years of SMAP observations (April 2015 – March 2020) and no longer rely on data from the Soil Moisture and Ocean Salinity (SMOS) mission. The Version 5 L4_SM algorithm also benefits from an updated calibration of the microwave radiative transfer model parameters. Moreover, the land surface modeling system underpinning the L4_SM algorithm uses an improved surface aerodynamic roughness length formulation. Furthermore, an error in the fitting procedure used for one of the topography-related functions in the Catchment model was corrected. This error potentially affected the simulation of soil moisture in about 2% of all land surface elements in previous versions. Finally, the Version 5 L4_SM algorithm includes major software infrastructure upgrades, including full compliance with the modular and extensible Earth System Modeling Framework, to facilitate future science algorithm development.

An analysis of the time-average surface and root zone soil moisture shows that the global pattern of arid and humid regions is captured by the Version 5 L4_SM estimates. Compared to Version 4, the Version 5 surface and root-zone soil moisture is generally slightly drier, owing primarily to a bug fix in the ensemble perturbations algorithm. The bug fix also removed an error in the long-term water balance of the Version 4 product, which did not close even after accounting for the (small) effect of the soil moisture analysis increments. Because of these climatological differences, the Version 4 and Version 5 products should *not* be combined into a single dataset for use in applications.

Results from the core validation site comparisons indicate that Version 5 of the L4_SM data product meets the self-imposed L4_SM accuracy requirement, which is formulated in terms of the root-mean square (RMS) error after removal of the long-term mean error, i.e., ubRMSE$\leq$0.04 m^3 m^{-3}, where the error is vs. the unknown true soil moisture. Computed directly against core site in situ measurements at the 9 km scale, the average unbiased RMS difference of the 3-hourly L4_SM data is 0.040 m^3 m^{-3} for surface soil moisture and 0.027 m^3 m^{-3} for root zone soil moisture. When factoring in the measurement error of the in situ data, the L4_SM product clearly meets the 0.04 m^3 m^{-3} ubRMSE requirement. The L4_SM estimates are an improvement compared to estimates from a model-only open loop (OL5030) simulation, which demonstrates the beneficial impact of the SMAP brightness temperature data. Overall, L4_SM surface and root zone soil moisture estimates are more skillful than OL5030 estimates, with statistically significant improvements for surface soil moisture R and anomaly R values (based on 95% confidence intervals). Results from comparisons of the L4_SM product to in situ measurements from more than 400 sparse network sites corroborate the core validation site results.

The instantaneous soil moisture analysis increments lie within a reasonable range and result in spatially smooth soil moisture analyses. The long-term mean soil moisture analysis increments make up only a small fraction of the water budget. The O-F residuals exhibit only small regional biases on the order of 1-3 K

between the (rescaled) SMAP brightness temperature observations and the L4_SM model forecast, which indicates that the assimilation system is reasonably unbiased. The globally averaged time series standard deviation of the O-F residuals is 5.5 K, which reduces to 3.5 K for the observation-minus-analysis (O-A) residuals, reflecting the impact of the SMAP observations on the L4_SM system. Regionally, the time series standard deviation of the normalized O-F residuals deviates considerably from unity, which indicates that regionally the L4_SM assimilation algorithm over- or underestimates the total (model and observation) error present in the system.

In summary, Version 5 of the L4_SM product is sufficiently mature and of adequate quality for distribution to and use by the larger science and application communities.

1 INTRODUCTION

The NASA Soil Moisture Active Passive (SMAP) mission provides global measurements of L-band (1.4 GHz) brightness temperature from a 685-km, near-polar, sun-synchronous orbit. These observations are primarily sensitive to soil moisture and temperature in the top few centimeters of the soil. SMAP data can therefore be used to enhance our understanding of processes that link the terrestrial water, energy, and carbon cycles, and to extend the capabilities of weather and climate prediction models (Entekhabi et al. 2014).

The suite of SMAP data products includes the Level 4 Surface and Root Zone Soil Moisture (L4_SM) product, which provides deeper-layer soil moisture estimates that are not available in the Level 2-3 retrieval products. The L4_SM product is based on the assimilation of SMAP brightness temperatures into the NASA Catchment land surface model (Koster et al. 2000) using a customized version of the Goddard Earth Observing System (GEOS) land data assimilation system (Figure 1; Reichle et al. 2014a, 2017a,b, 2019). This system, which is based on the ensemble Kalman filter (EnKF), accounts for model and observational uncertainty through perturbations of select Catchment model forcing and soil moisture prognostic variables, propagates the surface information from the SMAP instrument to the deeper soil, and ultimately provides global, 3-hourly estimates of soil moisture and other land surface fields without gaps in coverage. The publication latency of the L4_SM product is about 3 days. This latency is driven by the availability of the gauge-based precipitation product used to force the land surface model (Reichle and Liu 2014; Reichle et al. 2014b, 2017a,b, 2021).

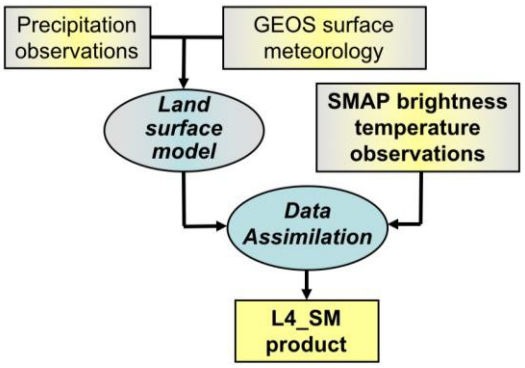

Figure 1. Schematic of the L4_SM algorithm.

The L4_SM product provides surface and root zone soil moisture (along with other geophysical fields) as 3-hourly, time-average fields on the global, cylindrical, 9 km Equal-Area Scalable Earth, version 2 (EASEv2) grid in the "geophysical" (or "gph") output Collection (Reichle et al. 2018a). Moreover, instantaneous soil moisture and soil temperature fields before and after the assimilation update are provided every three hours on the same grid in the "analysis update" (or "aup") output Collection, along with other assimilation diagnostics and error estimates. Time-invariant land model parameters, such as soil porosity, wilting point, and microwave radiative transfer parameters, are provided in the "land-model-constants" (or "lmc") Collection (Reichle et al. 2018a).

For geophysical data products that are based on the assimilation of satellite observations into numerical process models, validation is critical and must be based on quantitative estimates of uncertainty. Direct comparison with independent observations, including ground-based measurements, is a key part of validation. This assessment report provides a detailed description of the status of the L4_SM data quality for the Version 5 release of the L4_SM data product. The L4_SM validation process and data quality of previous versions are discussed by Reichle et al. (2015, 2016, 2017a,b, 2018b, 2019, 2021).

2 SMAP CALIBRATION AND VALIDATION OBJECTIVES

During the post-launch SMAP calibration and validation (Cal/Val) phase each science product team pursues two objectives:

1. Calibrate, verify, and improve the performance of the science algorithm.
2. Validate the accuracy of the science data product as specified in the science requirements and according to the Cal/Val schedule.

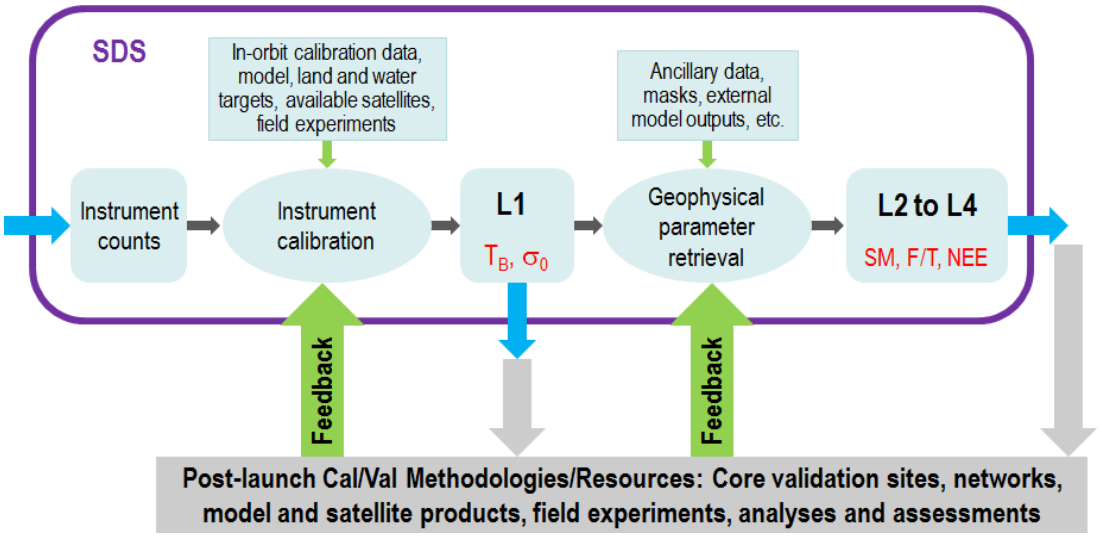

Figure 2. Overview of the SMAP calibration and validation process.

The overall SMAP Cal/Val process is illustrated in Figure 2. This process was first formalized in the SMAP Science Data Cal/Val Plan (Jackson et al. 2014) and the SMAP L2-L4 Data Products Cal/Val Plan (Colliander et al. 2014). Recently, many pioneering aspects of the SMAP Cal/Val process were incorporated into community standards for soil moisture product validation and good practices (Gruber et al. 2020; Montzka et al. 2020). The present assessment report describes how the L4_SM team addressed the Cal/Val objectives for the Version 5 release. The validation approach and procedures that apply specifically to the L4_SM product are further detailed in the Algorithm Theoretical Basis Document for the L4_SM data product (Reichle et al. 2014b).

SMAP established unified definitions to address the mission requirements. These are documented in the SMAP Handbook (Entekhabi et al. 2014), where calibration and validation are defined as follows:

- *Calibration*: The set of operations that establish, under specified conditions, the relationship between sets of values or quantities indicated by a measuring instrument or measuring system and the corresponding values realized by standards.
- *Validation:* The process of assessing by independent means the quality of the data products derived from the system outputs.

To ensure the public's timely access to SMAP data, the mission was required to release validated data products within one year of the beginning of mission science operations. The objectives and maturity of the SMAP validated release products follow the guidance provided by the Committee on Earth Observation

Satellites (CEOS) Working Group on Calibration and Validation (CEOS 2015), which can be summarized as follows (Colliander et al. 2021; their Appendix A):

- Stage 1 Validation: Product accuracy is assessed from a small (typically < 30) set of locations and time periods by comparison with in-situ or other suitable reference data.
- Stage 2 Validation: Product accuracy is estimated over a significant (typically > 30) set of locations and time periods by comparison with reference in situ or other suitable reference data. Spatial and temporal consistency of the product, and its consistency with similar products, has been evaluated over globally representative locations and time periods. Results are published in the peer-reviewed literature.
- Stage 3 Validation: Uncertainties in the product and its associated structure are well quantified over a significant (typically > 30) set of locations and time periods representing global conditions by comparison with reference in situ or other suitable reference data. Validation procedures follow community-agreed-upon good practices. Spatial and temporal consistency of the product, and its consistency with similar products, has been evaluated over globally representative locations and time periods. Results are published in the peer-reviewed literature.
- Stage 4 Validation: Validation results for stage 3 are systematically updated when new product versions are released and as the interannual time-series expands. When appropriate for the product, uncertainties in the product are quantified using fiducial reference measurements over a global network of sites and time periods (if available).

For the Version 5 release, the L4_SM team has completed Stages 1-4, including repeated publication of the latest validation results in the peer-reviewed literature (Reichle et al. 2017a,b, 2019, 2021; Colliander et al. 2021). The Cal/Val program will continue over the SMAP mission life span. Incremental improvements are ongoing as more measurements become available from the SMAP observatory. Version 5 data will be replaced in the archive when upgraded product versions become available.

3 L4_SM CALIBRATION AND VALIDATION APPROACH

During the mission definition and development phase, the SMAP Science Team and Cal/Val Working Group identified the metrics and methodologies that would be used for L2-L4 product assessment. These metrics and methodologies were vetted in community Cal/Val Workshops and tested in SMAP pre-launch Cal/Val rehearsal campaigns. The following validation methodologies and their general roles in the SMAP Cal/Val process were identified:

- *Core Validation Sites*: Accurate estimates at matching scales for a limited set of conditions.
- *Sparse Networks*: One point in the grid cell for a wide range of conditions.
- *Satellite Products*: Estimates over a very wide range of conditions at matching scales.
- *Model Products*: Estimates over a very wide range of conditions at matching scales.
- *Field Campaigns*: Detailed estimates for a very limited set of conditions.

Regarding the CEOS Cal/Val stages (section 2), core validation sites address Stage 1, and satellite and model products are used for Stage 2 and beyond. Sparse networks fall between these two stages.

For the L4_SM data product, all of the above methodologies can contribute to product assessment and refinement, but there are differences in terms of the importance of each approach for the validation of the L4_SM product.

The assessment of the L4_SM data product includes comparisons of SMAP L4_SM soil moisture estimates with in situ soil moisture observations from core validation sites and sparse networks. Moreover, independent soil moisture retrievals from satellite radar observations are used to measure the contribution of the SMAP analysis to the anomaly time series correlation skill of the L4_SM product across much of the global land surface. Finally, the assessment includes a global evaluation of the internal diagnostics from the ensemble-based data assimilation system that is used to generate the L4_SM product. This evaluation focuses on the statistics of the observation-minus-forecast (O-F) residuals and the analysis increments.

The core site comparisons, the assessment of the anomaly correlation skill using independent radar soil moisture retrievals, and the statistics of the assimilation diagnostics are considered primary validation methodologies for the L4_SM product. Comparisons against in situ measurements from regional-scale sparse networks are considered a secondary validation methodology because such in situ measurements are subject to upscaling errors from the point-scale to the grid-cell scale of the data product.

Due to their very limited spatial and temporal extent, data from field campaigns play only a tertiary role in the validation of the L4_SM data product. Note, however, that field campaigns are instrumental tools in the provision of high-quality, automated observations from the core validation sites and thus play an important indirect role in the validation of the L4_SM data product.

4 L4_SM ACCURACY REQUIREMENT

There is no formal Level 1 mission requirement for the validation of the L4_SM product, but the L4_SM team self-imposed an accuracy requirement mirroring the one applied to the L2_SM_AP product. Specifically, the L4_SM surface and root zone soil moisture estimates are required to meet the following criterion:

> **ubRMSE ≤ 0.04 m^3 m^{-3}** within the data masks specified in the *SMAP Level 2 Science Requirements* (that is, excluding regions of snow and ice, frozen ground, mountainous topography, open water, urban areas, and vegetation with water content greater than 5 kg m^{-2}),

where ubRMSE is the "unbiased" root-mean square (RMS) error, that is, the RMS error computed after removing long-term mean bias from the data (Entekhabi et al. 2010; Reichle et al. 2015, their Appendix A). (The ubRMSE is also referred to as the standard deviation of the error.) This criterion applies to the L4_SM instantaneous surface and root zone soil moisture estimates at the 9 km grid-cell scale from the "aup" Collection. It is verified by comparing the L4_SM product to the grid-cell scale in situ measurements from the core validation sites (section 6.2). The criterion applies to the site-average ubRMSE, which is obtained by averaging across the ubRMSE values for all 9 km core site reference pixels that provide suitable in situ measurements (Reichle et al. 2015).

L4_SM output fields other than instantaneous surface and root zone soil moisture are provided as research products (including surface meteorological forcing variables, soil temperature, evaporative fraction, net radiation, etc.) and will be evaluated against in situ observations to the extent possible given available resources.

As part of the validation process, additional metrics (including bias, RMS error, time series correlation coefficient R, and anomaly R values) are also computed for the L4_SM output. This includes computation of the metrics outside of the limited geographic area for which the ubRMSE≤0.04 m^3 m^{-3} validation criterion applies.

For the computation of the *anomaly* R metric, climatological values of soil moisture from a given dataset (i.e., the L4_SM product or the in situ measurements) at a given location are computed for each day of the year, thereby generating a local climatological seasonal cycle for that dataset. Anomaly time series are then computed by subtracting this climatological seasonal cycle from the corresponding raw data. The anomaly R metric is derived by computing the correlation coefficient between the L4_SM and the in situ anomaly time series (Reichle et al. 2015).

The validation includes additional metrics that are based on the statistics of the O-F residuals and other data assimilation diagnostics (section 6.5). Reichle et al. (2015) provide detailed definitions of all the validation metrics and confidence intervals used here.

5 L4_SM VERSION 5 RELEASE

5.1 Process and Criteria

Since the beginning of the SMAP science data flow on 31 March 2015, the L4_SM team has been conducting frequent assessments of the L4_SM data product and will continue to evaluate the product throughout the life of the SMAP mission. These assessments are based on core validation sites, sparse networks, and assimilation diagnostics, and they capture a wide range of geophysical conditions. The present report summarizes the status of this process.

The validation of the Version 5 L4_SM product includes comparisons against output from two model-only simulations that are based on the same land surface model and forcing data as the Version 5 L4_SM estimates but are not informed by SMAP brightness temperature observations (Table 1). Any accuracy in these model-only estimates is derived from the imposed meteorological forcing and land model structure and parameter information.

The first model-only simulation, the ensemble "open loop" (OL5030), employs 24 ensemble members and applies the same forcing and model prognostics perturbations that are also used in the Version 5 L4_SM algorithm, whereas the second model-only simulation, the "Nature Run," version 8.3 (NRv8.3), is a single-member land model simulation without perturbations (Table 1). The different characteristics of the ensemble open loop and the unperturbed simulation are exploited in section 6.1, where we assess the impact of the ensemble perturbations on the climatology of the L4_SM soil moisture estimates.

The OL5030 estimates were prepared for the SMAP period (31 March 2015 to present). The NRv8.3 estimates were generated for the period 1 January 2000 to present. In addition to serving as a reference in the L4_SM assessment, the NRv8.3 estimates also provide the modeled climatological information required by the L4_SM assimilation algorithm (Reichle et al. 2014b).

Table 1. Overview of L4_SM products and model-only simulations.

	No. ensemble members	Perturbations?	SMAP Assimilation?	Version 5	Version 4
L4_SM Product	24	Yes	Yes	Vv5030	Vv4030
Ensemble Open Loop	24	Yes	No	OL5030	OL4001
Nature Run	1	No	No	NRv8.3	NRv7.2

5.2 Processing and Science ID Version

The L4_SM product version used to prepare this assessment report has Science Version ID **Vv5030** (Table 1; Reichle et al. 2020a,b,c). The L4_SM Vv5030 algorithm assimilates operational data from the Version 5 SMAP L1C_TB brightness temperatures (CRID R17000 through 22 April 2021 and R17030 from 23 April 2021 through present; Chan et al. 2020).

The assessment period for this report is defined as the 6-year period from **1 April 2015, 0z to 1 April 2021, 0z**. The start date matches the first full day when the radiometer was operating under reasonably stable conditions following instrument start-up operations. The end date was selected to include the maximum possible number of full years at the time when the present report was prepared.

For illustrating select changes from the previous L4_SM product versions, this report also used published Version 4 L4_SM data (Science Version ID Vv4030; Reichle et al. 2018c,d,e), along with the corresponding Nature Run (NRv7.2) and ensemble open loop (OL4001) simulations (Table 1). Because Version 4 production ceased before the end of the 6-year validation period, direct comparisons of Version 4 and 5 data are conducted for the 4-year period from 1 April 2015, 0z to 1 April 2019, 0z.

Like previous versions, Version 5 of the L4_SM algorithm ingests only the SMAP L1C_TB radiometer brightness temperatures, contrary to the originally planned use of downscaled brightness temperatures from the L2_SM_AP product and landscape freeze-thaw state retrievals from the L2_SM_A product. The latter two products are based on SMAP radar observations and are only available for the 10-week period from 13 April to 7 July 2015 because of the failure of the SMAP radar instrument. The decision to use only radiometer (L1C_TB) inputs for the Version 5 release was made to ensure homogeneity in the longer-term L4_SM data record.

In February 2021, the SMAP Level-1 team discovered that errors in the antenna scan angle (ASA) inputs affected ~1,600 L1C_TB half-orbit data granules on 55 data-days in 2019 (5 October–23 November) and 2020 (4-5 February, 9 April, 30 May, and 18 June). The bad data exhibited geolocation errors up to ~100 km in the along-scan direction that were not identified by data quality flags. When the ASA errors were discovered, reprocessing of the L4_SM Vv5030 product was halted on data-day 4 October 2019 until nearly all of the 1,600 bad L1C_TB half-orbits were corrected. However, the processing of the published L4_SM Vv5030 data for October 2019 inadvertently used 22 of the bad L1C_TB half-orbits. To assess the impact of this processing error, we regenerated the Vv5030 L4_SM data for October 2019 under product counter 002 without ingesting the 22 bad L1C_TB half-orbits. The differences between the published Vv5030 data and the Vv5030 data with product counter 002 are minimal. There is virtually no impact on root-zone soil moisture, and the occasional differences in surface soil moisture dissipate very quickly. It is impossible to tell with a reasonable amount of effort whether the published or the product counter 002 data are more correct. For example, the antenna scan angle error might only impact the L1C_TB brightness temperature observations over ocean and ice; omitting the entire L1C_TB half-orbit from being used in L4_SM processing might then result in discarding good information over land. For these reasons, we decided **not** to replace the published Vv5030 data for October 2019 with the product counter 002 version. In the meantime, an automated check for ASA errors was added to L1C_TB processing by the Level-1 team and placed into operations on 23 April 2021 (CRID R17030). Future reprocessing of the L1C_TB and L4_SM data will therefore avoid a repeat of the aforementioned ASA processing errors.

5.3 Summary of Changes from Previous Version

This section provides a summary of algorithm changes between the previous L4_SM Version 4 algorithm and the current Version 5 assessed here.

Version 5 of the L4_SM algorithm uses the Catchment model version associated with NRv8.3, which includes minor updates from the previous version of the modeling system (NRv7.2). Specifically:

1.) NRv8.3 uses a revised formulation for the aerodynamic roughness length for consistency[1] with the land model version used in the currently operational version of the GEOS Forward-Processing

[1]Two differences between the land-related parameterizations in L4_SM and FP remain. Specifically, the Version 5 L4_SM algorithm uses the Louis surface turbulence scheme (Louis 1979) and vegetation (tree) height inputs derived from space-borne Lidar measurements (Simard et al. 2011), as in Version 4, whereas the current FP system uses the Helfand surface turbulence scheme (Helfand and Schubert, 1995) and old look-up table vegetation heights. The latter are used in FP because of a slight degradation in the medium-range forecast skill when the satellite-based vegetation heights were used in system development testing of the FP system (presumably owing to compensating errors). The L4_SM algorithm still uses the older Louis surface turbulence

(FP) system (Koster et al. 2020; Lucchesi 2018). The revised formulation includes a higher minimum surface roughness (which particularly affects turbulent fluxes in deserts) and applies estimates of stem area index along with leaf area index in the roughness calculation.

2.) NRv8.3 corrects an error in the fitting procedure used for one of the topography-related functions in the Catchment model, which potentially affects the simulation of soil moisture in about 2% of all land surface elements (De Lannoy et al. 2014b).

Moreover, the following changes impact the L4_SM brightness temperature analysis.

3.) The microwave radiative transfer parameters are calibrated following De Lannoy et al. (2013, 2014a). The parameters used in the Version 5 algorithm were calibrated using the matching NRv8.3 modeling system and 10 years of SMOS brightness temperature observations (July 2010 – June 2020).

4.) The calibration of the assimilated SMAP L1C_TB brightness temperatures changed substantially from Version 4 to Version 5. Over land, L1C_TB brightness temperatures are colder by 2-3 Kelvin on average in Version 5 compared to Version 4 (Peng et al. 2020). Consequently, the Version 5 L4_SM algorithm was recalibrated to work with the substantially changed calibration of the assimilated L1C_TB brightness temperatures. Specifically, the brightness temperature scaling parameters in the Version 5 L4_SM algorithm are based on five years of Version 5 SMAP brightness temperature observations (April 2015 – March 2020) and, unlike in previous versions, do not rely on SMOS data.

5.) A bug in the ensemble perturbations of the photosynthetically active radiation (PAR) forcing was fixed in the Version 5 L4_SM algorithm. In all previous L4_SM versions, this bug caused an error in the unstressed canopy resistance calculations, which resulted in an error in evapotranspiration primarily over arid regions and deserts, as well as a lack of closure of the water balance in these regions.

Finally, the Version 5 L4_SM algorithm includes major software infrastructure upgrades.

6.) Specifically, the Version 5 L4_SM algorithm is now fully compliant with the modular and extensible Earth System Modeling Framework (ESMF), to facilitate future science algorithm development.

7.) The solar zenith angle calculations in the Version 5 L4_SM algorithm use ESMF utilities, which differ slightly from the legacy code that was used in the Version 4 algorithm.

8.) In all previous L4_SM versions, there was a slight inconsistency in how ensemble averages of Catchment model diagnostic variables (such as soil moisture) were calculated. Specifically, the model diagnostic variables in the "Geophysical Data" (gph) output files were derived from the ensemble average of the model prognostic variables (such as the Catchment model soil water excess and deficit variables), whereas model diagnostic variables in the "Analysis Update Data" collection were first derived separately for each ensemble member and then averaged across the ensemble. In the Version 5 L4_SM algorithm, all model diagnostic outputs are first derived separately for each ensemble member and then averaged across the ensemble.

scheme because this scheme includes an implicit treatment of the sensitivity of aerodynamic resistance to both temperature and humidity; such a treatment is important in the offline (land-only) L4_SM modeling system but is not yet implemented in the newer Helfand scheme (Helfand and Schubert, 1995) used in the current FP system.

6 L4_SM DATA PRODUCT ASSESSMENT

This section provides a detailed assessment of the Version 5 L4_SM data product. First, global patterns and features are discussed briefly, including the impact of a bug in the ensemble perturbation algorithm in Version 4 that has been fixed in Version 5 (section 6.1). Next, we present comparisons and metrics versus in situ measurements from core validation sites (section 6.2) and sparse networks (section 6.3), followed by a brief discussion of the assessment versus satellite retrievals (section 6.4). Thereafter, we evaluate the assimilation diagnostics (section 6.5) through an analysis of the O-F brightness temperature residuals, the soil moisture increments, and the data product uncertainty estimates.

6.1 Global Patterns and Features

Figure 3 shows global maps of time-averaged Version 5 L4_SM surface and root zone soil moisture for the 6-year validation period (April 2015 – March 2021). The global patterns are as expected – arid regions such as the southwestern US, the Sahara Desert, the Arabian Peninsula, the Middle East, southern Africa, and central Australia exhibit generally dry surface and root zone soil moisture conditions, whereas the tropics (Amazon, central Africa, and Indonesia) and high-latitude regions show wetter conditions.

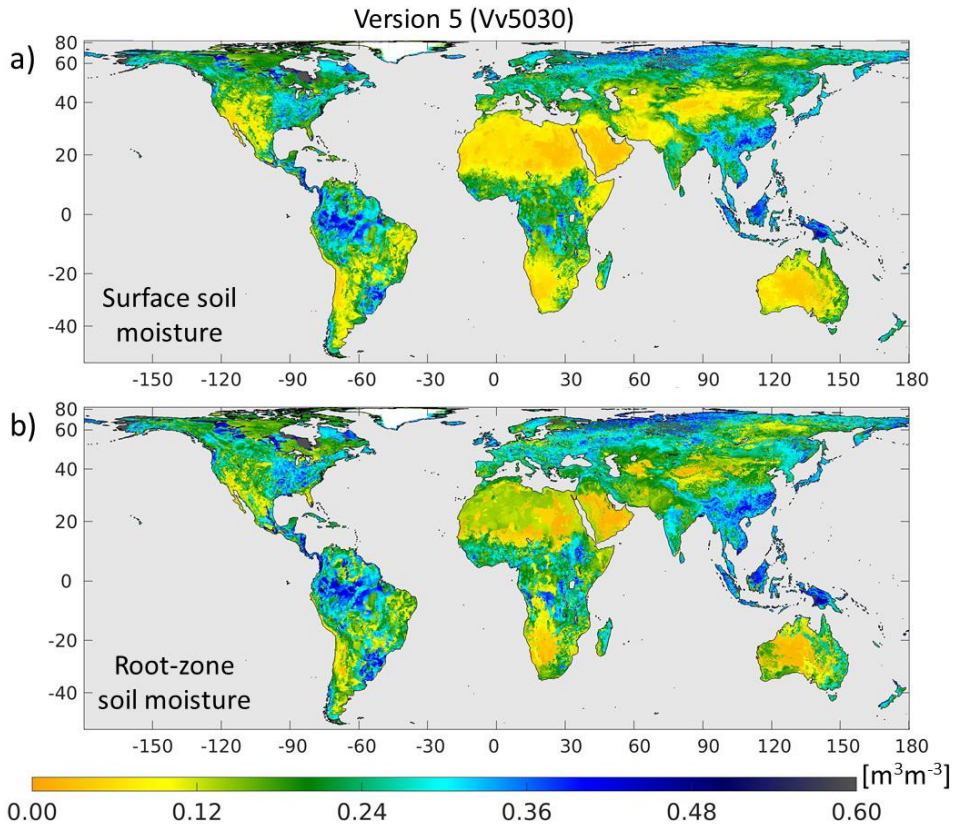

Figure 3. Time-average of Version 5 L4_SM (a) surface and (b) root zone soil moisture for April 2015 – March 2021. White shading indicates no-data-values (e.g., over the Greenland ice sheet).

Generally, the global patterns of absolute soil moisture values are dominated by soil parameters and climatological factors. The influence of soil texture is noticeable in the coarse-scale patterns in the Sahara Desert, where little is in fact known about the spatial distribution of mineral soil fractions. Areas with peat soil include, for example, the region along the southern edge of Hudson Bay and portions of Alaska. In the land model, the soils in this region are assigned a high porosity value and show persistently wetter conditions than seen in other areas.

Figure 4 shows global maps of the change in time-averaged soil moisture fields between the Version 4 and 5 L4_SM products for the 4-year period April 2015 – March 2019. Generally, the long-term mean soil moisture in Version 5 is slightly drier than in Version 4, by 0.008 m^3 m^{-3} in the global average for both surface and root-zone soil moisture. As will be explained in the following, these differences are the result of a complex interplay of the changes between Versions 4 and 5, listed in section 5.3 above.

First, the revised aerodynamic roughness length formulation and the slight changes in the solar zenith angle calculations (items 1 and 7 of section 5.3) have only a minor impact on the mean surface and root-zone soil moisture, which can be seen in the difference between the underlying NRv8.3 and NRv7.2 model-only simulations shown in Figure 5a,c. The curve fitting bug fix (item 2 of section 5.3) can result in larger differences locally, but these changes are limited to a small fraction of isolated tiles and are therefore not noticeable in Figure 5a,b.

The primary reasons for the mean soil moisture differences between the Version 4 and 5 L4_SM products (Figure 4) are related to the perturbations used in the ensemble data assimilation system. Specifically, spatio-temporally correlated perturbations are applied to the surface meteorological forcing data and the Catchment model soil moisture prognostic variables such that the spread in the ensemble simulation provides a reasonable representation of the model uncertainty (Reichle et al. 2017a).

The mean soil moisture differences between the Version 4 and 5 ensemble open loop simulations (Figure 5b,d) very closely resemble those between the Version 4 and 5 L4_SM products (Figure 4), which must therefore be related to the above-mentioned fixes of the PAR perturbations bug and the slightly inconsistent ensemble averaging order (items 5 and 8 of section 5.3). This also implies that the mean soil moisture differences between the Version 4 and 5 products are *not* driven by the L1C_TB and RTM calibration changes (items 3 and 4 of section 5.3), which have at most a minor impact on the mean soil moisture. (Section 6.5.2 below shows that the already small long-term mean soil moisture analysis increments of Version 4 have been further reduced in magnitude in Version 5.)

Further insights can be gained by examining the impact of the perturbations on the long-term mean soil moisture in the modeling system. Figure 6 shows, separately for each version, the mean surface and root-zone soil moisture differences between the ensemble open loop and unperturbed model-only simulations (see also Table 1). As expected, in both versions the soil moisture perturbations result in increased mean surface and root-zone soil moisture in arid and semi-arid regions, where soil moisture is generally so dry that perturbations can often only add but not remove water. Elsewhere, however, the perturbations have a net drying effect on surface soil moisture (Figure 6a,b). The most striking discrepancy between Versions 4 and 5 is in the mean root-zone soil moisture differences between the ensemble open loop and unperturbed model simulations (compare Figure 6c,d). In Version 4, the ensemble open loop root-zone soil moisture is wetter than the unperturbed simulation across much of the globe, which is a direct consequence of the PAR perturbations bug (item 5 of section 5.3). Fixing this bug in Version 5 brings the mean root-zone soil moisture of the ensemble open loop much closer to that of the unperturbed simulation.

Further investigation revealed that the ensemble average of the perturbed precipitation forcing is smaller by ~0.5% than that of the unperturbed precipitation (Figure 7a), resulting in generally drier surface soil moisture when perturbations are used. This small precipitation deficit is caused when the standard-normal deviates, which are generated with an ensemble mean of zero and with outliers limited to 2.5 times the standard deviation, are nonlinearly converted into lognormal space for use in the multiplicative precipitation perturbations. Similarly, the ensemble average of the multiplicatively perturbed downward

shortwave radiation forcing is ~0.2% less than without perturbations (Figure 7b). Less shortwave forcing, however, should result in reduced evapotranspiration and thus wetter surface soil moisture conditions. Outside of arid and semi-arid regions and for the perturbation parameter settings employed in the L4_SM algorithm, the precipitation deficiency dominates and explains the slightly drier surface soil moisture conditions seen in the Version 5 ensemble open loop compared to the unperturbed simulation (Figure 6b). Generally, the gap between the mean of the (multiplicatively) perturbed forcing and the unperturbed forcing increases with increasing standard deviation of the perturbations and with tighter restrictions on outliers (not shown). When the threshold for outliers is relaxed to 3 times the standard deviation, the nonlinear effect becomes negligible. (Applying the threshold for outliers in lognormal space would require different thresholds for low and high outliers, owing to the strong asymmetry of the lognormal distribution.)

Additionally, in the high latitudes and in high-elevation arid environments (including the Atacama Desert and the Tibetan Plateau), the ensemble average of the perturbed downward longwave radiation forcing differs by ~1-5 W m^{-2} from that of the unperturbed simulation (Figure 7c). This discrepancy is caused by an air temperature-radiation consistency check that is applied to the (perturbed) longwave radiation. This check is based on the Stefan-Boltzmann equation and pre-specified values for the minimum and maximum permissible emissivities of 0.5 and 1.0, respectively. In the more extreme high-latitude and high-elevation environments, the perturbed longwave radiation is frequently reset to fall within the permissible range, thereby causing the discrepancy between the ensemble average of the perturbed downward longwave radiation and its unperturbed nominal value.

The surface soil moisture difference between the ensemble open loop and the unperturbed simulation in the Version 4 modeling system (Figure 6a) can now be understood as the superposition of the artificially increased soil wetness caused by the PAR perturbations bug (seen in Figure 6c for root-zone soil moisture) and the wet/dry difference pattern caused by the nonlinear effects in the perturbations algorithm (seen in Figure 6b for the Version 5 modeling system).

Finally, Figure 8 shows the long-term soil water balance residuals for Versions 4 and 5. The water balance residual is computed as $(S_f - S_i)/\Delta t - (P - ET - R) - \Delta I$, where S_f and S_i are the final and initial total soil water storage, Δt is the averaging time interval (April 2015 – March 2019), P is the mean precipitation, ET is the mean evapotranspiration, R is the mean total runoff, and ΔI is the mean profile soil moisture analysis increment (in flux units). As can be seen in Figure 8a, the water balance did not close in the Version 4 L4_SM product. This lack of closure was primarily a consequence of the PAR perturbations bug, which caused inconsistent values of the unstressed canopy resistance term and thus erroneous ET values. This error has been fixed in the Version 5 system (Figure 8b).

In summary, Figures 6 and 8 clearly show that Version 5 is more consistent than Version 4 mainly for two reasons: (i) the ensemble average of the perturbed simulation is closer to the unperturbed simulation in Version 5 compared to Version 4 and (ii) the water balance closure violation seen in Version 4 has been removed in Version 5.

Because of the climatological differences in soil moisture (Figure 4), the Version 4 and Version 5 products should *not* be combined into a single dataset for use in applications.

The L4_SM product also includes many output fields that are not subject to formal validation requirements. Such "research" output includes the surface meteorological forcing fields, land surface fluxes, soil temperature and snow conditions, runoff, and error estimates (derived from the ensemble). See Reichle et al. (2015, their section 6.1) for more discussion of the global patterns and features found in the L4_SM product.

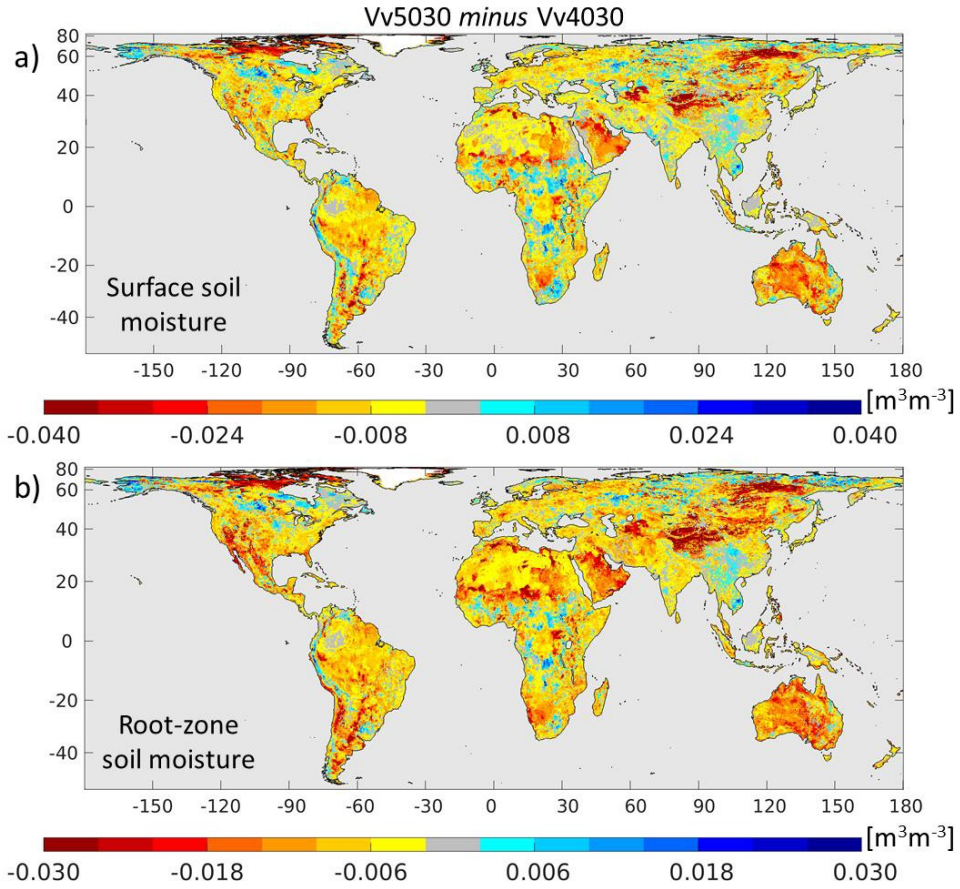

Figure 4. As in Figure 3 but for Version 5 minus Version 4 and April 2015 – March 2019.

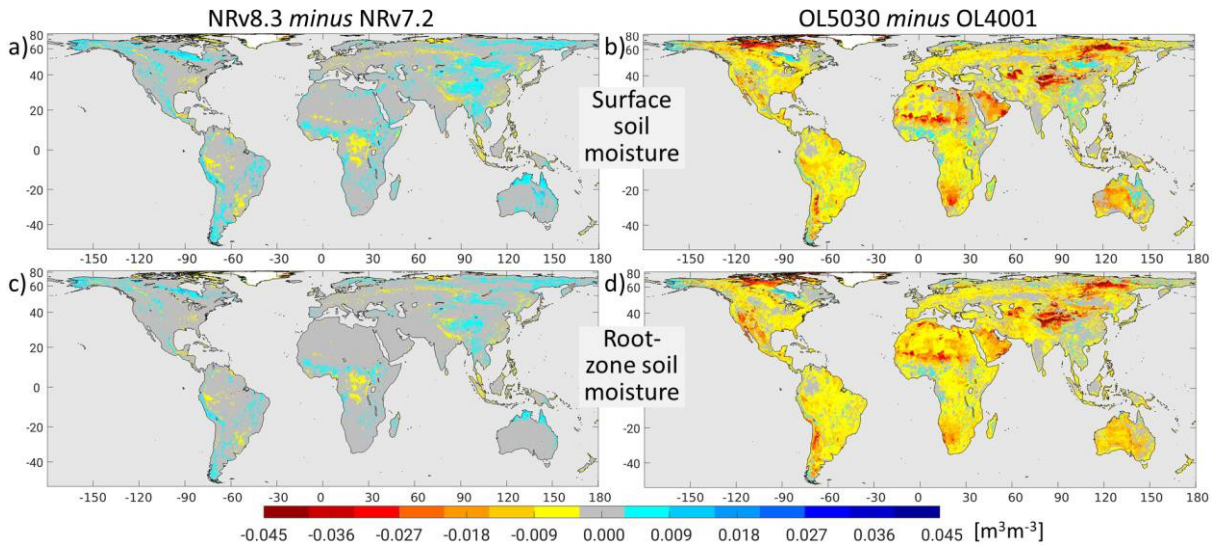

Figure 5. Time-average soil moisture differences between the Version 5 and Version 4 modeling systems: (a,b) surface and (c,d) root-zone soil moisture differences between (a,c) the unperturbed NRv8.3 and NRv7.2 simulations and (b,d) the OL5030 and OL4001 ensemble open loop simulations for April 2015 – March 2019. White shading indicates no-data-values.

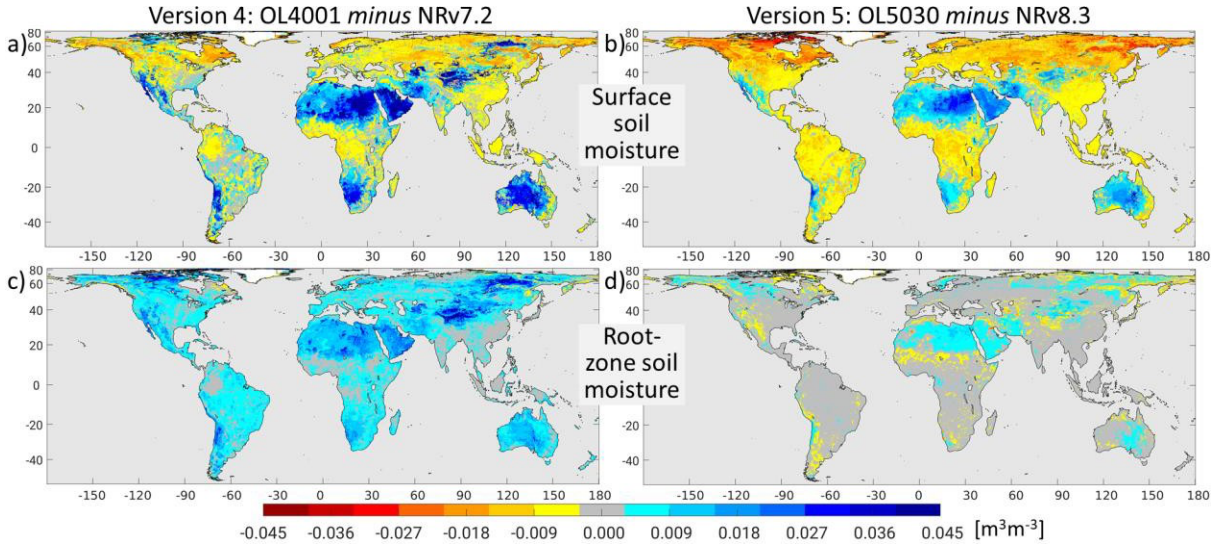

Figure 6. Time-average soil moisture differences between ensemble open loop and unperturbed simulations: (a,b) surface and (c,d) root-zone soil moisture difference between (a,c) OL4001 and NRv7.2 (Version 4) and (b,d) OL5030 and NRv8.3 (Version 5) for April 2015 – March 2019. White shading indicates no-data-values.

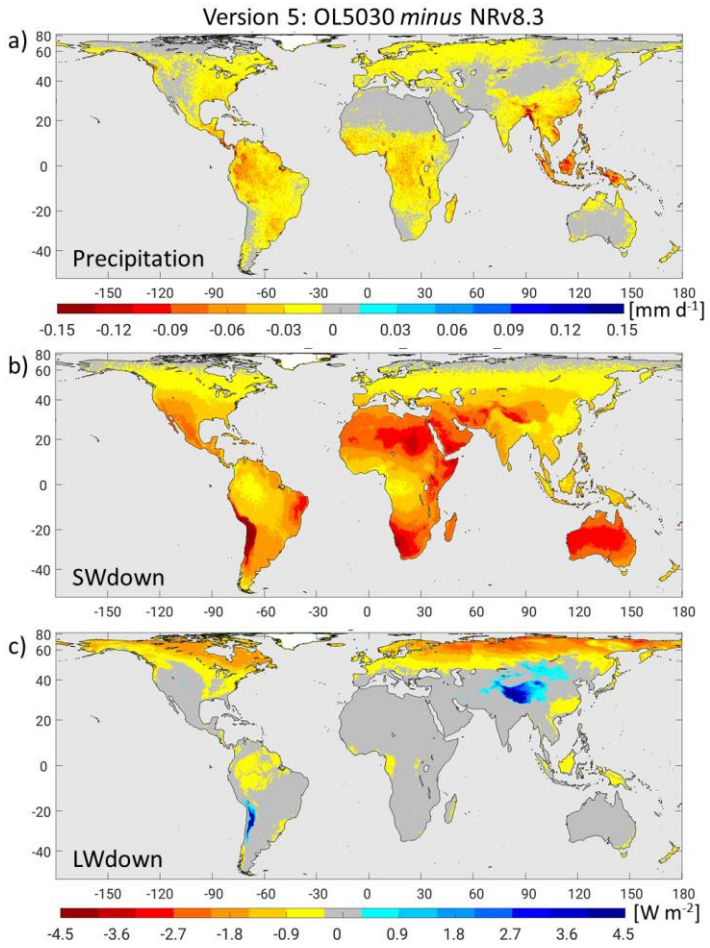

Figure 7. Time-average surface meteorological forcing difference between the ensemble mean of the open loop (OL5030) simulation and the unperturbed (NRv8.3) simulation for (a) total precipitation (b) downward shortwave radiation, and (c) downward longwave radiation for April 2015 – March 2019. The bottom colorbar applies to both (b) and (c). White shading indicates no-data-values.

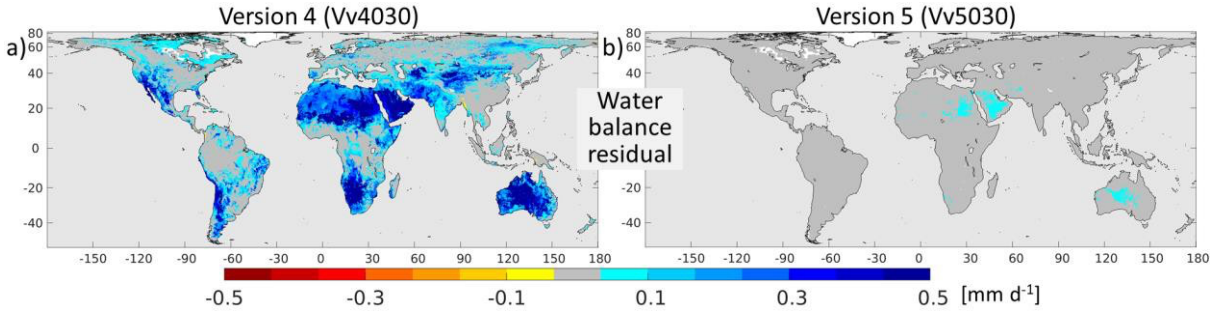

Figure 8. Time-average soil water balance residual of the (a) Version 4 and (b) Version 5 L4_SM product for April 2015 – March 2019. White shading indicates no-data-values. In Version 4, the water balance did not close owing to a bug in the radiation forcing perturbations (see text for details).

6.2 Core Validation Sites

6.2.1 Method

This section provides an assessment of the L4_SM soil moisture estimates using data from SMAP core validation sites, which provide in situ measurements of soil moisture conditions at the scale of 9 km and 33 km grid cells (Colliander et al. 2017a,b). Like the L4_SM Version 4 assessment (Reichle et al. 2018b, 2019), this report uses reference pixel data on the 33 km EASEv2 grid (defined through suitable aggregation of the 3 km EASEv2 grid), instead of the 36 km reference pixels used in earlier assessments (Reichle et al. 2015, 2016, 2017a). Additional details about the processing of the data and the validation methodology can be found in Reichle et al. (2015, their section 6.2.1).

The status of the core validation sites is reviewed periodically. The set of core sites that provide data for this assessment of the L4_SM product are listed in Table 2, along with the details of the 9 km and 33 km reference pixels that are used. The list of core sites matches that of the Version 4 assessment, but there are a couple of minor changes in the list of references pixels (Table 3). The present (Version 5) L4_SM validation is based on a total of 48 reference pixels from 19 different core validation sites. Surface soil moisture measurements are available for all 48 reference pixels, which include 18 reference pixels at the 33 km scale from 18 different sites and 30 reference pixels at the 9 km scale from 18 different sites. For root zone soil moisture, measurements are available for only 19 reference pixels from 8 different core sites, including 8 reference pixels at the 33 km scale from 8 different sites and 12 reference pixels at the 9 km scale from 7 different sites. The 9 km reference pixels for root zone soil moisture belong to the core validation sites of Little Washita (Oklahoma), Fort Cobb (Oklahoma), Little River (Georgia), South Fork (Iowa), Tonzi Ranch (California), Kenaston (Saskatchewan), and TxSON (Texas). The same 7 sites plus Yanco (Australia) provide root zone soil moisture data at the 33 km scale. This very limited set obviously lacks the diversity to be fully representative of global conditions, but we are not aware of any other comparable datasets.

The metrics are computed from 3-hourly data, provided at least 480 measurements, or about 2 months of data, are available after quality control. The computation of the anomaly R value (section 4) further requires estimates of the 6-year mean seasonal cycle, for which we required a minimum of at least 240 measurements for a given 31-day smoothing window across the 6-year validation period. This requirement implies that the anomaly R metric is available for surface (root zone) soil moisture at only 17 (7) reference pixels at the 33 km scale. At the 9 km scale, the anomaly R metric is available whenever the other metrics are also available.

Table 3 also lists the depths of the deepest sensors that contribute to the in situ root zone soil moisture measurements. The measurements from the individual sensors are vertically averaged with weights that are proportional to the spacing of the depth of the sensors within the 0-100 cm layer depth of the L4_SM root zone soil moisture estimates. At all reference pixels except Little River and Yanco, the deepest sensors are at 40-50 cm depth. At Little River and Yanco, the deepest sensors are at 30 cm and 75 cm, respectively, with Yanco's second-deepest sensors being installed at 45 cm depth. In all cases, the deepest sensors are therefore weighted most strongly in the computation of the vertical average. To compute the vertically averaged root zone soil moisture at a given time from a given sensor profile, all sensors within the profile must provide measurements that pass the automated quality control.

Table 2. Soil moisture core validation sites used in the present assessment.

Site Name	*Country*	*Climate Regime*	*Land Cover*	*Number of 9-km (33-km) Reference Pixels*		*Reference*
				Surface Soil Moisture	*Root-zone Soil Moisture*	
REMEDHUS	Spain	Temperate	Croplands	2 (1)	- (-)	Sanchez et al. 2012; Gonzalez-Zamora et al. 2015
Reynolds Creek	USA (Idaho)	Arid	Grasslands	2 (1)	- (-)	Seyfried et al. 2001
Yanco	Australia (New South Wales)	Arid	Cropland / natural mosaic	2 (1)	- (1)	Panciera et al. 2014
Carman	Canada (Manitoba)	Cold	Croplands	1 (1)	- (-)	McNairn et al. 2015
Ngari	Tibet	Cold	Barren / sparse	- (1)	- (-)	Wen et al. 2014
Walnut Gulch	USA (Arizona)	Arid	Shrub open	3 (1)	- (-)	Keefer et al. 2008
Little Washita	USA (Oklahoma)	Temperate	Grasslands	3 (1)	2 (1)	Cosh et al. 2006
Fort Cobb	USA (Oklahoma)	Temperate	Grasslands	2 (1)	2 (1)	Cosh et al. 2014
Little River	USA (Georgia)	Temperate	Cropland / natural mosaic	1 (1)	1 (1)	Bosch et al. 2007
St Josephs	USA (Indiana)	Temperate	Croplands	1 (1)	- (-)	Heathman et al. 2012
South Fork	USA (Iowa)	Cold	Croplands	3 (1)	3 (1)	Coopersmith et al. 2015
Monte Buey	Argentina	Temperate	Croplands	1 (1)	- (-)	Thibeault et al. 2015
Tonzi Ranch	USA (California)	Temperate	Savannas woody	1 (1)	1 (1)	Clewley et al. 2017; Moghaddam et al. 2016
Kenaston	Canada (Saskatchewan)	Cold	Croplands	2 (1)	1 (1)	Rowlandson et al. 2015; Tetlock et al. 2019
Valencia	Spain	Cold	Savannas woody	1 (-)	- (-)	Juglea et al. 2010; Khodayar et al. 2019
Niger	Niger	Arid	Grassland	1 (1)	- (-)	Galle et al. 2018
Benin	Benin	Tropical	Savannas	1 (1)	- (-)	Galle et al. 2018
TxSON	USA (Texas)	Temperate	Grasslands	2 (1)	2 (1)	Caldwell et al. 2018
HOBE	Denmark	Temperate	Croplands	1 (1)	- (-)	Bircher et al. 2012; Jensen and Refsgaard 2018
All Sites				***30 (18)***	***12 (8)***	

Table 3. Soil moisture core validation site reference pixels used in the present assessment. The 33 km reference pixels are shown in boldface. See Table 2 for core validation site characteristics.

Site Name (Abbreviation)	Reference Pixel										
	ID	Latitude [degree]	Longitude [degree]	Horizontal Scale [km]	Depth of Deepest Sensor [m]	Number of Sensors (Surface Soil Moisture)			Number of Sensors (Root Zone Profiles)		
						Min.	Mean	Max.	Min.	Mean	Max.
REMEDHUS (RM)	**03013302**	**41.29**	**-5.46**	**33**	**0.05**	**8**	**12.3**	**15**	n/a	n/a	n/a
	03010903	41.42	-5.37	9	0.05	4	4.0	4	n/a	n/a	n/a
	03010908	41.32	-5.27	9	0.05	4	4.0	4	n/a	n/a	n/a
Reynolds Creek (RC)	**04013302**	**43.19**	**-116.75**	**33**	**0.05**	**7**	**7.0**	**7**	n/a	n/a	n/a
	04010907	43.19	-116.72	9	0.05	4	4.0	4	n/a	n/a	n/a
	04010910	43.09	-116.81	9	0.05	4	4.0	4	n/a	n/a	n/a
Yanco (YC)	**07013301**	**-34.86**	**146.16**	**33**	**0.75**	**8**	**19.5**	**23**	**7**	**14.9**	**23**
	07010902	-34.72	146.13	9	0.05	8	8.6	9	n/a	n/a	n/a
	07010916	-34.98	146.31	9	0.05	8	10.1	11	n/a	n/a	n/a
Carman (CR)	**09013301**	**49.60**	**-97.98**	**33**	**0.05**	**8**	**18.0**	**20**	n/a	n/a	n/a
	09010906	49.67	-97.98	9	0.05	8	9.9	11	n/a	n/a	n/a
Ngari (NG)	**12033301**	**32.50**	**79.96**	**33**	**0.05**	**6**	**6.0**	**6**	n/a	n/a	n/a
Walnut Gulch (WG)	**16013302**	**31.75**	**-110.03**	**33**	**0.05**	**8**	**15.4**	**18**	n/a	n/a	n/a
	16010906	31.72	-110.09	9	0.05	8	9.2	11	n/a	n/a	n/a
	16010907	31.72	-109.99	9	0.05	8	10.0	11	n/a	n/a	n/a
	16010913	31.83	-110.90	9	0.05	6	6.0	6	n/a	n/a	n/a
Little Washita (LW)	**16023302**	**34.86**	**-98.08**	**33**	**0.45**	**8**	**10.7**	**12**	**8**	**9.0**	**12**
	16020905	34.92	-98.23	9	0.05	4	4.0	4	n/a	n/a	n/a
	16020906	34.92	-98.14	9	0.45	4	4.0	4	4	4.0	4
	16020907	34.92	-98.04	9	0.45	4	4.0	4	4	4.0	4
Fort Cobb (FC)	**16033302**	**35.38**	**-98.64**	**33**	**0.45**	**8**	**10.4**	**11**	**8**	**9.5**	**11**
	16030911	35.38	-98.57	9	0.45	4	4.0	4	4	4.0	4
	16030916	35.29	-98.48	9	0.45	4	4.0	4	4	4.0	4
Little River (LR)	**16043302**	**31.67**	**-83.60**	**33**	**0.30**	**8**	**17.1**	**19**	**8**	**15.6**	**18**
	16040901	31.72	-83.73	9	0.30	8	8.0	8	6	6.3	8
St Josephs (SJ)	**16063302**	**41.39**	**-85.01**	**33**	**0.05**	**8**	**8.3**	**9**	n/a	n/a	n/a
	16060907	41.45	-84.97	9	0.05	7	7.0	7	n/a	n/a	n/a
South Fork (SF)	**16073302**	**42.42**	**-93.41**	**33**	**0.50**	**8**	**17.6**	**19**	**8**	**12.4**	**16**
	16070909	42.42	-93.53	9	0.50	4	4.0	4	4	4.0	4
	16070910	42.42	-93.44	9	0.50	4	4.0	4	4	4.0	4
	16070911	42.42	-93.35	9	0.50	4	4.0	4	4	4.0	4
Monte Buey (MB)	**19023301**	**-32.91**	**-62.51**	**33**	**0.05**	**8**	**9.9**	**12**	n/a	n/a	n/a
	19020902	-33.01	-62.49	9	0.05	5	5.0	5	n/a	n/a	n/a
Tonzi Ranch (TZ)	**25013301**	**38.45**	**-120.95**	**33**	**0.40**	**8**	**13.1**	**20**	**8**	**14**	**10**
	25010911	38.43	-120.95	9	0.40	8	15.0	26	8	18	12
Kenaston (KN)	**27013301**	**51.47**	**-106.48**	**33**	**0.50**	**8**	**27.0**	**30**	**8**	**23.8**	**30**
	27010910	51.39	-106.51	9	0.05	8	8.0	8	n/a	n/a	n/a
	27010911	51.39	-106.42	9	0.50	8	13.0	14	8	11.7	14
Valencia (VA)	41010906	39.57	-1.26	9	0.05	7	7.0	7	n/a	n/a	n/a
Niger (NI)	**45013301**	**13.57**	**2.66**	**33**	**0.05**	**6**	**6.0**	**6**	n/a	n/a	n/a
	45010902	13.57	2.66	9	0.05	4	4.0	4	n/a	n/a	n/a
Benin (BN)	**45023301**	**9.83**	**1.73**	**33**	**0.05**	**7**	**7.0**	**7**	n/a	n/a	n/a
	45020902	9.77	1.68	9	0.05	5	5.0	5	n/a	n/a	n/a
TxSON (TX)	**48013301**	**30.35**	**-98.73**	**33**	**0.50**	**8**	**28.8**	**29**	**8**	**23.8**	**24**
	48010902	30.43	-98.81	9	0.50	8	9.9	10	8	8.9	10
	48010911	30.28	-98.73	9	0.50	8	15.0	15	8	13.9	14
HOBE (HB)	**67013301**	**55.97**	**9.10**	**33**	**0.05**	**8**	**11.2**	**15**	n/a	n/a	n/a
	67010901	55.97	9.10	9	0.05	5	5.0	5	n/a	n/a	n/a

Across the reference pixels listed in Table 3, the average number of individual surface soil moisture sensors that contribute to a given 33 km reference pixel ranges between 6.0 and 28.8, with a mean value of 13.6. The corresponding number of sensor profiles for root zone soil moisture ranges between 9.0 and 23.8, with a mean value of 15.4. At the 9 km scale, 13 of the 31 reference pixels are based on just 4 individual sensor profiles, while most of the rest of the 9 km reference pixels consist of about 10 sensor profiles each. The mean value of surface soil moisture sensors per 9 km reference pixel is 6.8, and the corresponding number of root zone profiles is 7.2. The sampling density (sensors per unit area) is therefore higher for the 9 km reference pixels than for the 33 km reference pixels.

For most reference pixels, individual sensor profiles occasionally drop out temporarily. If the sensor that drops out is installed in a particularly wet or a particularly dry location (relative to reference pixel average conditions), not having this sensor contribute to the reference pixel average will result in an artificial discontinuity in the time series of the reference pixel average soil moisture. In previous assessment reports, this effect was mitigated only for reference pixels with 8 or fewer individual sensor profiles; for these reference pixels, quality-controlled in situ measurements from all contributing sensor profiles needed to be available for the computation of the reference pixel average.

The processing of the in situ measurements for the present assessment report includes an additional safeguard against discontinuities caused by temporary sensor dropout. In the revised processing used here, the time series from each individual sensor is first converted from volumetric soil moisture units into standard-normal deviates, based on the time series mean and variance of the measurements at the individual sensor. Next, a normalized reference pixel average time series is computed by averaging the standard-normal deviate time series from each individual sensor. Finally, the resulting normalized reference pixel average time series is converted back into volumetric units based on the reference pixel average of the soil moisture climatologies from the individual sensors. By averaging the measurements from the individual sensors in the normalized space, the reference pixel average time series in volumetric units is less sensitive to the dropping out of sensors that are installed in a particularly wet or dry location (relative to reference pixel average conditions).

Core site metrics are provided separately for the 9 km and 33 km reference pixels. Metrics are computed directly against the (reference pixel average) in situ measurements. Because the latter contain measurement error, we present the metrics as the mean *difference* (MD), RMS *difference* (RMSD), and unbiased RMS *difference* (ubRMSD), along with the (anomaly) correlation. Because of the in situ measurement error, the metrics of interest – that is, the (absolute) bias, RMSE, and ubRMSE – are less than the (absolute) MD, RMSD, and ubRMSD, respectively. Similarly, the (anomaly) correlation vs. the true soil moisture exceeds the (anomaly) correlation that is directly determined against the imperfect in situ measurements.

Summary metrics are obtained by averaging across the metrics from all individual reference pixels at the given scale (Table 3). For the 9 km metrics, we first average each metric across the 9 km reference pixels within each site, separately for each site and weighted by the number of measurements that contribute to the metric at a given 9 km reference pixel. Second, we average the resulting individual site-average metrics across all sites. This approach gives equal weight to each site and differs from the straight average over all 9 km reference pixels that was used in earlier assessments (Reichle et al. 2015, 2016, 2017a), which somewhat arbitrarily gave more weight to sites that had more 9 km reference pixels. (We computed summary metrics using both methods and found the results to be close. That is, the conclusions remain the same regardless of how exactly the average metric is computed.)

Finally, in situ measurements are used for validation only when the model (or assimilation) estimates indicate non-frozen and snow-free conditions (Reichle et al. 2015, their section 6.2.1). Because the soil temperature and snow states differ somewhat between the L4_SM product and the model-only (Open Loop) simulation examined here, in situ measurements were used only if both datasets indicate favorable

validation conditions. This cross-masking ensures that the metrics are directly comparable across both datasets.

6.2.2 Results

In this section, we investigate the summary metrics for soil moisture at the core validation sites, which are illustrated in Figures 9 and 10. Probably the most important result is that the average ubRMSE for surface and root zone soil moisture for the Version 5 L4_SM product at both the 9 km and the 33 km scales meets the accuracy requirement of ubRMSE ≤ 0.04 m^3 m^{-3}.

For a more in-depth analysis, we first compare the skill of the L4_SM (Vv5030) product to that of the model-only Open Loop (OL5030) estimates. For the ubRMSD metrics at the 9 km and the 33 km scales (Figure 9a), the surface and root zone soil moisture skill of the Version 5 product slightly exceeds that of OL5030, demonstrating the positive impact of assimilating SMAP brightness temperatures. For example, at the 9 km scale the surface soil moisture ubRMSD is 0.040 m^3 m^{-3} for Vv5030 surface soil moisture and 0.042 m^3 m^{-3} for OL5030. However, the ubRMSD improvement of the L4_SM product over the model-only simulation is not statistically significant at the 5% level, as indicated by the overlapping 95% confidence intervals. (Note that the confidence intervals are themselves uncertain and only provide rough guidance.)

When factoring in the measurement error of the reference pixel-average in situ observations, which Chen et al. (2019) conservatively estimate as ubRMSE~0.01-0.02 m^3 m^{-3}, the Version 5 L4_SM product clearly meets the above-mentioned accuracy requirement.

The average MD (Figure 9b) and average absolute MD (Figure 9c) values for surface and root zone soil moisture tend to be slightly worse for the Version 5 product than for the model-only (OL5030) estimates. The differences in the MD metrics are again not statistically significant and are in any case much smaller than the upscaling uncertainty (Chen et al. 2019).

Across-the-board improvements are seen in the L4_SM product over the model-only Open Loop estimates in terms of R (Figure 10a) and anomaly R (Figure 10b) skill. The improvements range from 0.04 to 0.13 and are statistically significant for surface soil moisture at both the 9 km and 33 km scales.

Next, we compare the skill values at 9 km to those at 33 km. The L4_SM and Open Loop skill values at 33 km are better for all metrics than the corresponding values at 9 km (Figures 9 and 10), which is consistent with the fact that the model forcing data and the assimilated SMAP brightness temperature observations are all at resolutions of about 30 km or greater. The information used to downscale the assimilated information primarily stems from the land model parameters, which are at the finer, 9 km resolution; this information is expected to have a modest impact at best. It is therefore not a surprise that the estimates at 33 km are more skillful than those at 9 km.

Finally, we compare the skill of the surface estimates to that of the root zone estimates. Across both scales, for nearly all metrics and for both the L4_SM and Open Loop estimates, the skill of the root zone soil moisture estimates is better than that of the surface estimates. This result makes sense because there is much more variability in surface soil moisture. It is important to keep in mind, however, that the root zone metrics are computed from only a subset of the sites used for the computation of the surface metrics.

Generally, the results presented here, which are based on up to 6 years of core site measurements, are consistent with those of the Version 4 product and model-only estimates, which were based on a validation period of 3 years (Reichle et al. 2017a). In summary, the results discussed here demonstrate that Version 5 of the L4_SM product is of sufficient maturity and quality for dissemination to the public.

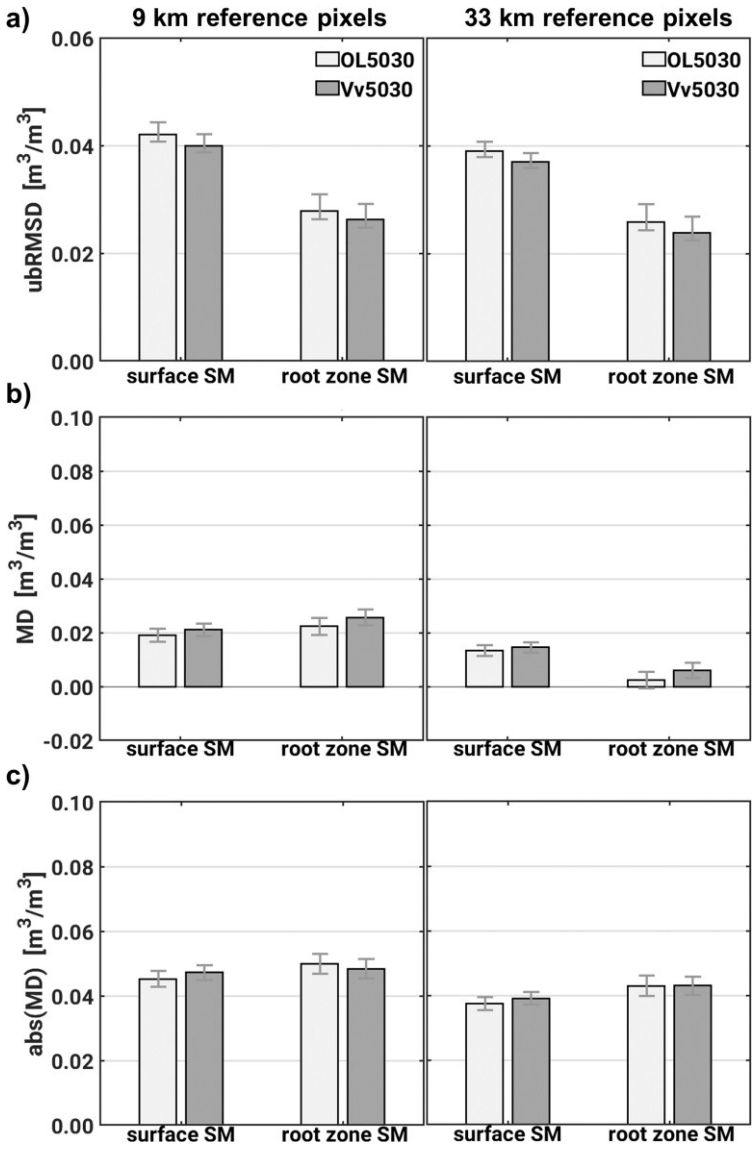

Figure 9. Surface and root zone soil moisture (a) ubRMSD, (b) MD and (c) absolute MD averaged across (left) 9 km and (right) 33 km core site reference pixels for Version 5 Open Loop (OL5030) estimates and the Version 5 L4_SM (Vv5030) product.

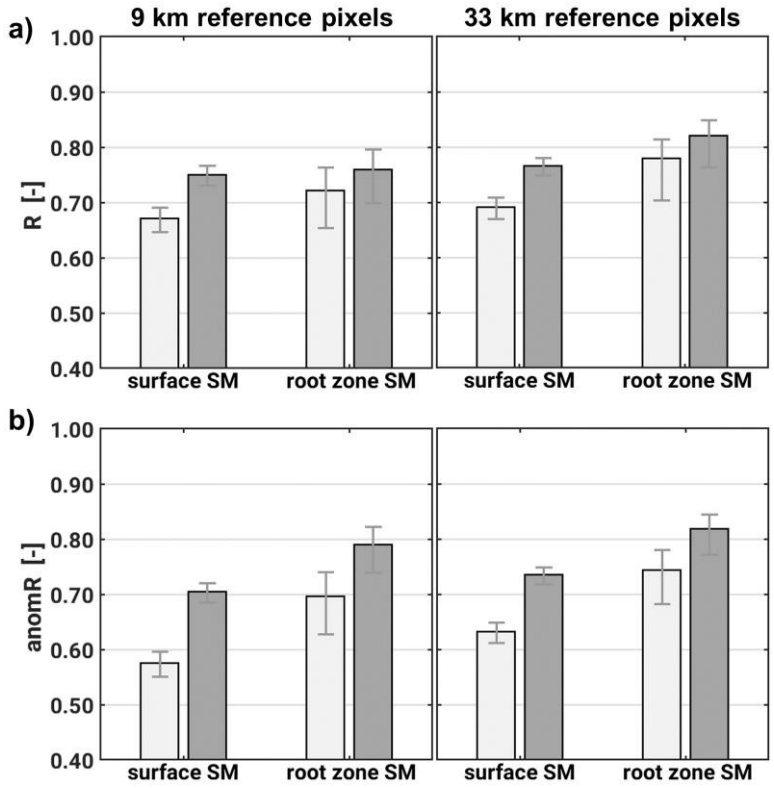

Figure 10. As in Figure 9 but for (a) time series correlation coefficient (R) and (b) anomaly R.

6.3 Sparse Networks

6.3.1 Method

The locally dense networks of the core validation sites are complemented by regional to continental-scale "sparse" networks. The defining feature of the sparse networks is that there is usually just one sensor (or profile of sensors) located within a given 9 km EASEv2 grid cell. Such point-scale measurements are, of course, generally not representative of the grid cell average conditions that the L4_SM algorithm is trying to estimate. Although sparse networks are not ideal for soil moisture validation for this and other reasons, they offer in situ measurements in a larger variety of environments and provide data quasi-operationally with very short latency. See Reichle et al. (2015) for further discussion of the advantages and limitations of using sparse networks in the L4_SM validation process.

This assessment report focuses on metrics obtained from a direct comparison of the L4_SM product to in situ measurements, that is, metrics derived without using triple collocation approaches that attempt to correct for errors in the in situ measurements (Chen et al. 2016; Gruber et al. 2016). The values of the time series correlation metrics provided here are thus lower than those that would be obtained with the aid of triple collocation, and they are therefore conservative estimates of the true skill. Note also that the *relative* performance of the products under investigation does not depend on the use of triple collocation approaches (Dong et al. 2020).

The skill of the L4_SM estimates was computed using all available in situ measurements (after quality control) at 3-hourly time steps, and this skill was compared to that of the model-only Open Loop estimates. For sparse networks, we used the same requirements for the minimum number of data values as for core validation sites (section 6.2). Note that quality control generally excludes in situ measurements when the ground is frozen (see Reichle et al. 2015, Appendix C). Instantaneous L4_SM data from the "aup" Collection and corresponding Open Loop data were taken directly from the standard 9 km EASEv2 grid cell that includes the sensor location (that is, the data product estimates are not interpolated bilinearly or otherwise to the precise location of the in situ sensor locations). Metrics were computed for surface and root zone soil moisture against in situ measurements from the SCAN, USCRN, OK Mesonet, OZNet-Murrumbidgee, and SMOSMania networks (Table 4). The average metrics were computed based on a clustering algorithm that assigns the weights given to each location based on the density of sites in the surrounding region (De Lannoy and Reichle 2016).

Table 4. Overview of sparse networks, with indication of the sensor depths, number of sites, and data periods used here. Values in parentheses indicate the number of sites for which the anomaly R metric was computed. The anomaly R metric was only available for sites with sufficient data to compute a seasonally varying climatology. Count of USCRN (OK Mesonet) sites includes 4 (1) site(s) with undetermined IGBP land cover classification.

Network	Region	Sensor Depths (m)	Number of Sites				Period (MM/DD/YYYY)	Reference
			Surface		Root Zone			
SCAN	USA	0.05, 0.10, 0.20, 0.50	135	(134)	109	(107)	04/01/2015 - 03/31/2021	Schaefer et al. 2007
USCRN	USA	0.05, 0.10, 0.20, 0.50	111	(111)	78	(76)	04/01/2015 - 03/31/2021	Bell et al. 2013; Diamond et al. 2013
OK Mesonet	Okla. USA	0.05, 0.25, 0.60	118	(116)	77	(76)	04/01/2015 - 05/01/2018	McPherson et al. 2007
OZNet	Australia	0.04, 0.45	43	(43)	19	(19)	04/01/2015 - 09/01/2020	Smith et al. 2012
SMOSMania	France	0.05, 0.20	21	(21)	21	(21)	04/01/2015 - 12/31/2019	Calvet et al. 2007
All Networks			***428***	***(425)***	***304***	***(299)***		

Measurements used for L4_SM validation cover most of the contiguous United States (SCAN, USCRN, OK Mesonet), parts of the Murrumbidgee basin in Australia (OZNet), and an area in south-western France (SMOSMania). The in situ measurements from the sparse network sites were subjected to extensive automated and manual quality control procedures by the L4_SM team following (Liu et al. 2011), which removed spikes, temporal inhomogeneities, oscillations, and other artifacts that are commonly seen in these automated measurements. In our experience, the manual inspection and quality control is an indispensable step in the process. Table 4 also lists the number of sites with sufficient data after quality control.

A total of 428 sites provided surface soil moisture measurements, and 304 provided root zone soil moisture measurements. Most of the sites are in the continental United States, including about 100 each in the USCRN and SCAN networks, and another ~100 sites in Oklahoma alone from the OK Mesonet. The OZNet network contributes 43 sites with surface soil moisture measurements, of which 19 sites also provide root zone measurements. Finally, 21 sites with surface and root zone soil moisture measurements were used from the SMOSMania network. For most networks, around ~30% of the sites do not have sufficient numbers of measurements for the computation of the climatology that is needed to determine the anomaly R skill.

Table 4 also lists the sensor depths that were used to compute the in situ root zone soil moisture. As with the core validation sites, vertical averages for SCAN, USCRN, and OK Mesonet are weighted by the spacing of the sensor depths within the 0-100 cm layer corresponding to the L4_SM estimates, and the

average is only computed if all sensors within a given profile provide measurements after quality control. For SCAN and USCRN sites, some measurements at 100 cm depth are available, but these deeper layer measurements are not of the quality and quantity required for L4_SM validation and are therefore not used here. For OZNet and SMOSMania, in situ root zone soil moisture is given by the measurements at the 45 cm and 20 cm depth, respectively; that is, no vertical average is computed.

6.3.2 Results

Figure 11 shows the average L4_SM and Open Loop metrics across all sparse network sites. When validated against the sparse network measurements, both versions of the L4_SM products show generally lower ubRMSD and higher R and anomaly R values than the corresponding Open Loop estimates, with improvements that are statistically significant at the 5% level for the surface soil moisture correlation metrics. This again demonstrates the additional information contributed by the assimilation of the SMAP brightness temperature observations in the L4_SM system.

As with the core site validation results, the ubRMSD and MD values vs. the sparse network measurements are smaller (better) for root zone soil moisture than for surface soil moisture, which again reflects the fact that root zone soil moisture generally varies less in time than surface soil moisture.

As with the core validation sites, the validation of the L4_SM and Open Loop estimates vs. sparse network measurements is within regions where the surface meteorological forcing takes advantage of high-quality, gauge-based precipitation measurements. Larger improvements from the assimilation of SMAP observations can be expected in areas where the CPCU precipitation product is based on fewer gauges.

Overall, the evaluation of skill for the sparse network sites yields results that are very similar to those obtained for the core validation sites. The beneficial impact of assimilating SMAP brightness temperature observations is greatest for surface soil moisture, with smaller improvements in root zone soil moisture estimates. Finally, it is important to keep in mind that all of the skill metrics presented here underestimate the true skill because these metrics are based on a direct comparison against in situ measurements (which are subject to error). Therefore, the sparse network ubRMSD values suggest that the L4_SM estimates would meet the formal accuracy requirement across a very wide variety of surface conditions, beyond those that are covered by the relatively few core validation sites that have been available to date for formal verification of the accuracy requirement. One caveat, however, is that the sparse network results do not provide an entirely independent validation because SCAN and USCRN measurements were used to calibrate an earlier version (NRv7.2) of the model (Reichle et al. 2018b). Nevertheless, the sparse network results provide additional confidence in the conclusions drawn from the core validation site comparisons.

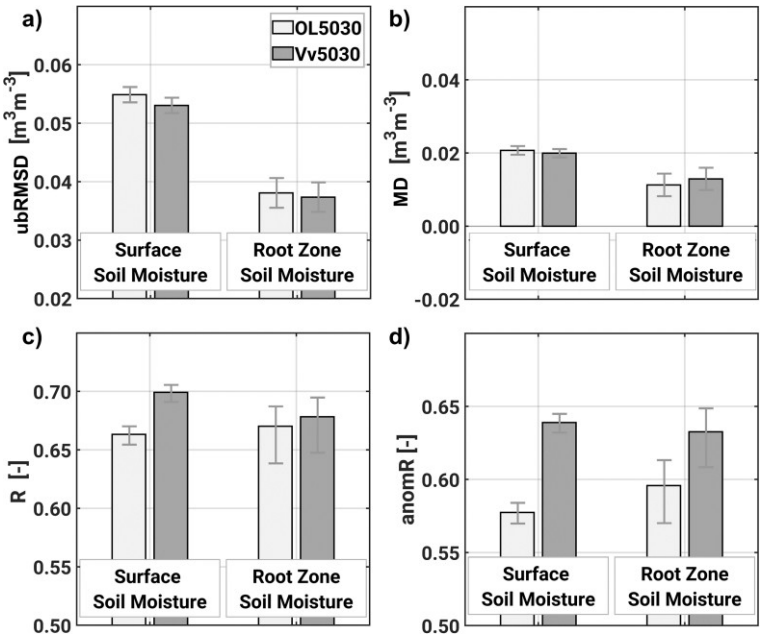

Figure 11. Skill metrics for Version 5 Open Loop (OL5030) estimates and the Version 5 L4_SM product (Vv5030) over the sparse network sites listed in Table 4. (a) ubRMSD, (b) MD, (c) time series correlation coefficient (R), and (d) anomaly R.

6.4 Satellite Soil Moisture Retrievals

Reichle et al. (2021) quantified the contribution of the SMAP brightness temperature analysis to the anomaly time series correlation skill of the L4_SM product based on the instrumental variable (IV) method and independent soil moisture retrievals from the Advanced Scatterometer (ASCAT; Wagner et al. 2013), an active microwave (radar) instrument. In a nutshell, the IV method obtains the difference in skill (vs. the unknown true soil moisture) between the L4_SM and model-only estimates through the respective sample correlation skill values vs. the independent ASCAT satellite observations. Reichle et al. (2021) validated the ASCAT-based IV approach at the SMAP core validation sites using the grid cell-scale in situ measurements (their Figure 4). For the Version 4 L4_SM product, Reichle et al. (2021) find that, in the global average, the SMAP brightness temperature analysis increases the surface soil moisture anomaly correlation by 0.11 (their Figure 5b), compared to an increase of just 0.03 from the CPCU-based precipitation corrections (their Figure 5c). The contrast is particularly strong in central Australia, where the CPCU precipitation product is known to have considerable errors and O-F brightness temperature residuals are larger when CPCU precipitation is used.

For the present report, we repeated the Reichle et al. (2021) assessment using the Version 5 L4_SM product. The improvement in the anomaly correlation of the Version 5 L4_SM product over the model-only (OL5030) estimates is very similar to that seen in Version 4 (Reichle et al. 2021; their Figure 5b). Moreover, the global mean of the anomaly correlation skill between the Version 4 and 5 L4_SM products is unchanged. Consequently, the graphics for the Version 4 system presented by Reichle et al. (2021) still apply to Version 5 and are therefore not repeated here.

6.5 Data Assimilation Diagnostics

This section provides an evaluation of the L4_SM data assimilation diagnostics, including the statistics of the observation-minus-forecast (O-F) residuals, the observation-minus-analysis (O-A) residuals, and the analysis increments. Because the L4_SM algorithm assimilates brightness temperature observations, the O-F and O-A diagnostics are in terms of brightness temperatures (that is, in "observation space"). The analysis increments are, strictly speaking, in the space of the Catchment model prognostic variables that make up the "state vector", including the "root zone excess", "surface excess", and "top-layer ground heat content" (Reichle et al. 2014b). For the discussion below, the soil moisture increments have been converted into equivalent volumetric soil moisture content in units of $m^3\ m^{-3}$ and into water flux terms in units of mm d^{-1}.

A key element of the analysis update is the downscaling and inversion of the observational information from the 36 km grid of the assimilated brightness temperatures into the modeled geophysical variables on the 9 km grid, based on the modeled error characteristics, which vary dynamically and spatially. An example and illustration of a single analysis update can be found in Reichle et al. (2017b, their section 3b).

6.5.1 Observation-Minus-Forecast Residuals

Figure 12 shows the total number of L1C_TB observations that were assimilated at each grid cell in Version 5 during the assessment period (April 2015 – March 2021). This count includes H- and V-pol observations from ascending and descending orbits. The average data count across the globe is approximately 2,361 for the 6-year (2,192-day) period. The corresponding (3-year) map for Version 4 is very similar (Reichle et al. 2019, their Figure 5a). Few or no SMAP brightness temperatures are assimilated in high-elevation and mountainous areas (including the Rocky Mountains, the Andes, the Himalayas, and Tibet), in the vicinity of lakes (such as in northern Canada), and next to major rivers (including the Amazon and the Congo). In the high latitudes, the much shorter warm (unfrozen) season also results in lower counts of assimilated brightness temperature observations, although this is somewhat mitigated by SMAP's polar orbit, which results in more frequent revisit times there. The remaining gaps in coverage might reflect a lack of sufficient numbers of SMAP observations to provide the required climatological information for the computation of the (seasonally varying) brightness temperature scaling parameters during the times of the year when conditions are suitable for a soil moisture analysis. Note, however, that the L4_SM product provides soil moisture estimates everywhere, even if in some regions the L4_SM estimates are not based on the assimilation of SMAP observations and rely only on the information in the model and forcing data.

Next, Figure 13 shows the global distributions of the time series mean and standard deviation of the O-F brightness temperature residuals. The time mean values of the O-F residuals are typically small and mostly range from -3 to 3 K, with an overall bias of just 0.06 K and a mean absolute bias of just 0.29 K (Figure 13a). The latter represents a reduction of about 50% from the (3-year) mean absolute bias of 0.56 K seen in the Version 4 system (Reichle et al. 2019, their Figure 6a) and reflects the improved Version 5 algorithm calibration (section 5.3).

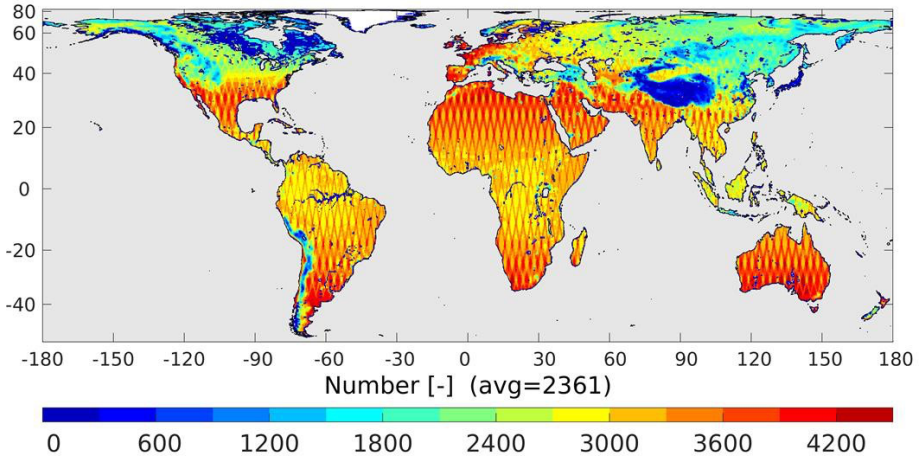

Figure 12. Number of L1C_TB observations used in the L4_SM algorithm (Vv5030) during the 6-year validation period (April 2015 – March 2021). Data counts include H-pol and V-pol data from ascending and descending half-orbits. White shading indicates no-data-values.

The time series standard deviation of the O-F residuals ranges from a few Kelvins to around 15 K (Figure 13b). The highest values are found in central North America, southern South America, southern Africa, the Sahel, central Asia, India, and (particularly) Australia. These regions have sparse or modest vegetation cover and typically exhibit strong variability in soil moisture conditions. The O-F residuals are generally smallest in more densely vegetated regions, including the eastern United States, the Amazon basin, and tropical Africa. Small values are also found in the high latitudes, including Alaska and Siberia, and in the Sahara Desert. The global (spatial) average of the O-F standard deviation is 5.5 K in Version 5, which is less than the (3-year) value of 5.7 K in Version 4 (Reichle et al. 2019, their Figure 7a) and suggests that the Version 5 modeling system is slightly better able to predict the observed brightness temperatures just prior to each analysis. The spatially averaged time series standard deviation of the O-A residuals is 3.5 K (not shown), which again reflects the impact of the SMAP observations in the L4_SM system.

Finally, Figure 14 shows the standard deviation of the *normalized* O-F residuals, which measures the consistency between the expected (modeled) errors and the actual errors. Specifically, the O-F residuals are normalized with the standard deviation of their expected total error, which is the sum (in a covariance sense) of the error in the observations (including instrument errors and errors of representativeness) and the error in the brightness temperature model forecasts (Reichle et al. 2015, their Appendix B). The parameters that determine the expected error standard deviations are key inputs to the ensemble-based L4_SM assimilation algorithm. If they are chosen such that the expected errors are fully consistent with the actual errors, the metric shown in Figure 14 should be unity everywhere. If the metric is less than one, the actual errors are overestimated by the assimilation system, and if the metric is greater than one, the actual errors are underestimated.

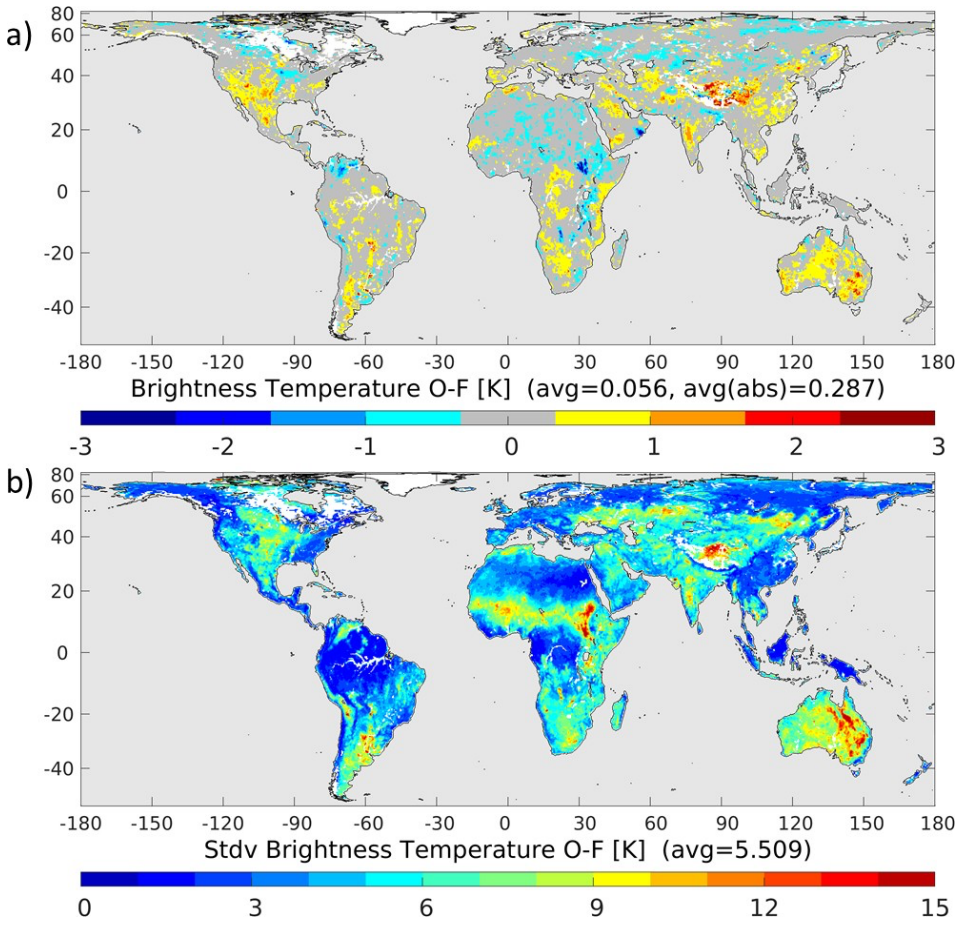

Figure 13. (a) Mean and (b) standard deviation of the O-F residuals from the L4_SM algorithm (Vv5030) for April 2015 – March 2021. White shading indicates no-data-values.

The global average of the metric in Version 5 is 1.07, which suggests that, on average, the modeled errors are slightly underestimating the actual errors (Figure 14). The metric, however, varies greatly across the globe. Typical values are either too low or too high. In the Amazon basin, the eastern US, tropical Africa, and portions of the high northern latitudes, values are around 0.5, and thus errors there are considerably overestimated. Conversely, in central North America, the Sahel, southern Africa, India, portions of central Asia and most of Australia, values range from 1.5 to 3, meaning that errors in these regions are considerably underestimated. In Version 4, the global pattern of low and high values of the normalized O-F standard deviation was very similar, but with a global average metric of 1.13 (Reichle et al. 2019, their Figure 8a). That is, the slight underestimation of the actual errors in Version 5 represents an improvement from that of Version 4. More work is needed to further improve the calibration of the input parameters that determine the model and observation errors in the L4_SM system.

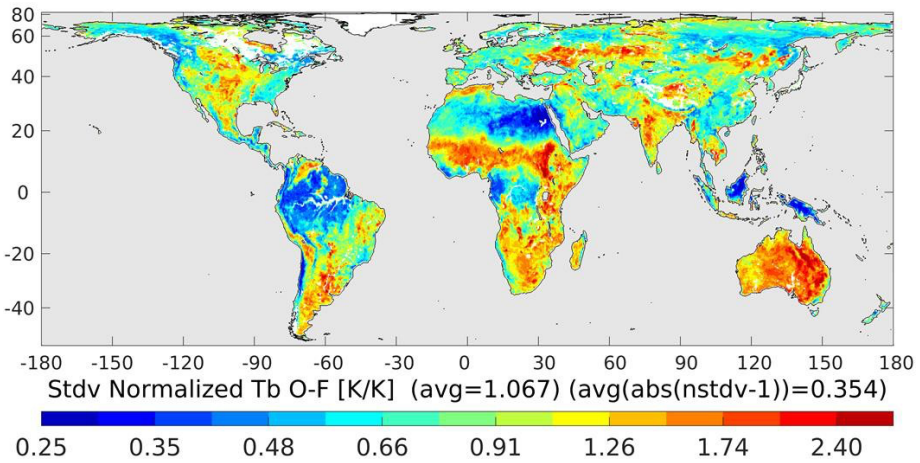

Figure 14. Standard deviation of the *normalized* O-F residuals from the L4_SM algorithm (Vv5030) for April 2015 – March 2021. White shading indicates no-data-values.

6.5.2 Increments

Figure 15 shows the average number of increments that the L4_SM algorithm generated per day during the validation period. The global mean is 0.77 per day, which means that there are approximately four increments applied every five days on average, either from an ascending or a descending overpass. The overall pattern of the increments count follows that of the count of the assimilated observations shown in Figure 12. The figure also reveals the diamond patterns resulting from SMAP's regular 8-day repeat orbit. The corresponding (3-year) map for Version 4 is very similar (Reichle et al. 2019, their Figure 5c).

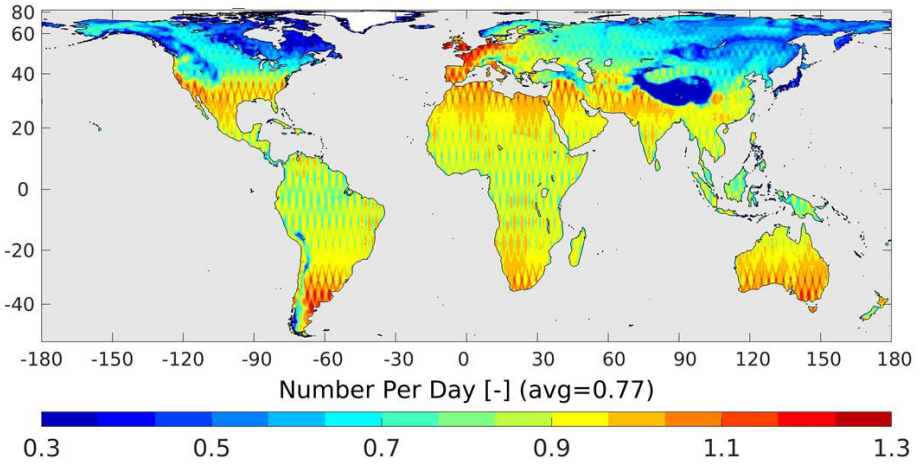

Figure 15. Average number of increments per day generated by the L4_SM algorithm (Vv5030) during the validation period (April 2015 – March 2021). The result applies equally to all elements of the control vector, including the model prognostic variables related to surface soil moisture, root zone soil moisture, surface temperature, and top-layer soil temperature. White shading indicates no-data-values.

Next, Figure 16 shows the time mean values of the analysis increments for surface and root zone soil moisture. In the global average, the net increments are only -0.012 mm d^{-1} for surface soil moisture and

0.017 mm d^{-1} (or ~6 mm per year) for root zone soil moisture. Regionally, however, the mean increments can be larger and constitute a non-negligible fraction of the water balance. The average absolute increment is about 0.030 mm d^{-1} for surface soil moisture and 0.055 mm d^{-1} for root zone soil moisture. For surface soil moisture, the central US, eastern South America, southeastern Africa, India, portions of central Asia, and southeastern Australia experience net drying increments in surface soil moisture, whereas central Australia experiences net wetting increments. The spatial pattern is different for root zone soil moisture increments, which have a net wetting effect in the central US, eastern South America, and all of Australia and a net drying effect in the eastern US, western and central Africa, and southeast Asia. Generally, the pattern of the net surface soil moisture increments reflects the long-term mean bias in the O-F residuals (Figure 13a). The long-term mean increments in Version 5 are typically smaller by a factor of two than those in Version 4 (not shown), which again reflects the improved calibration of the Version 5 algorithm (section 5.3).

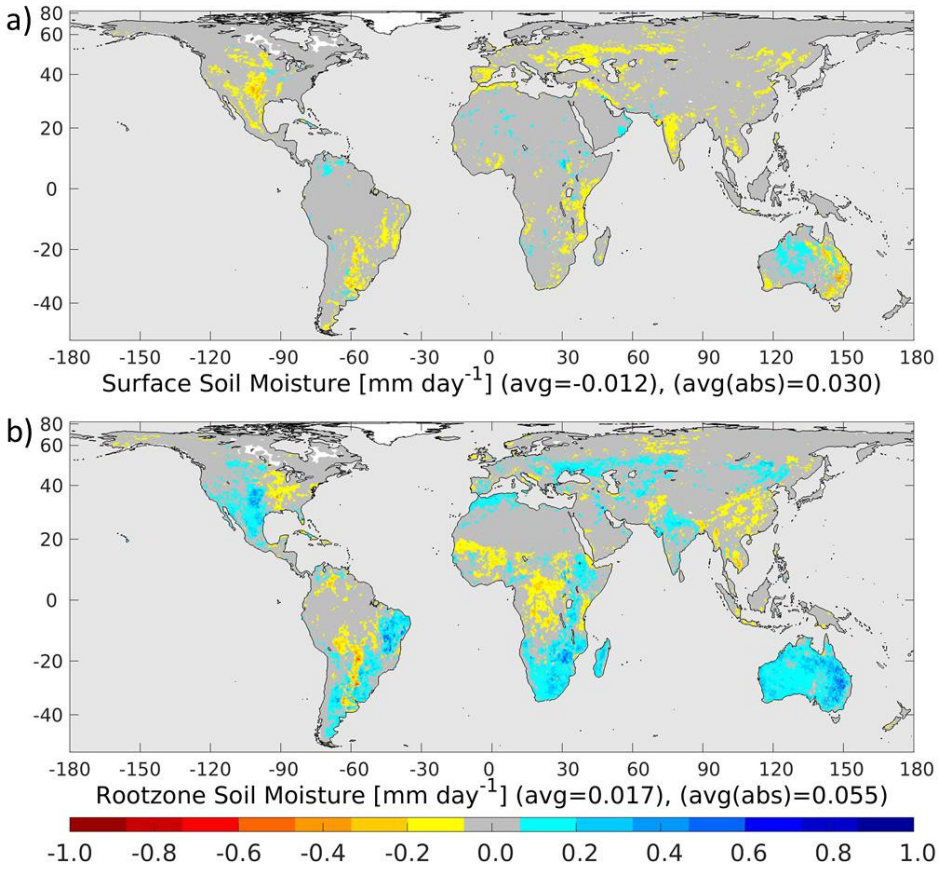

Figure 16. Time series mean of the increments for (a) surface soil moisture and (b) root zone soil moisture from the L4_SM algorithm (Vv5030) for Apr 2015 – March 2021 in equivalent flux units (mm d^{-1}). White shading indicates no-data-values.

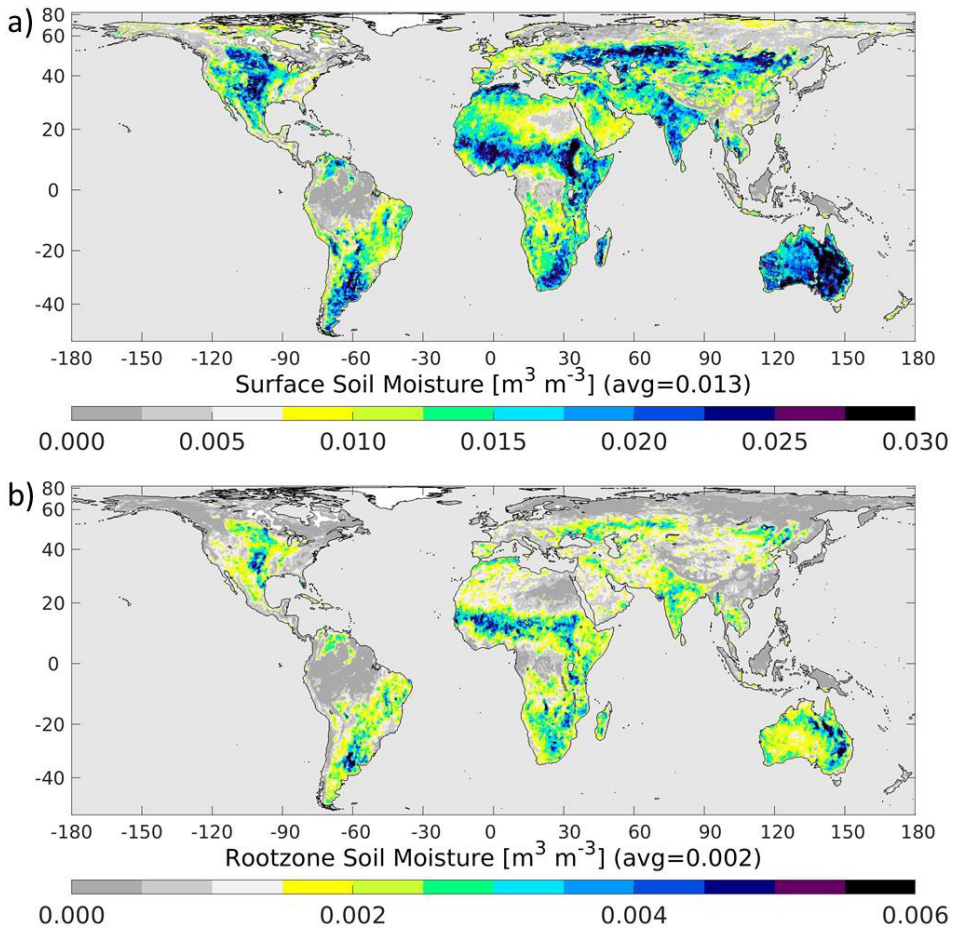

Figure 17. As in Figure 16 but for time series standard deviation of the increments in units of m^3 m^{-3}.

Finally, Figure 17 shows the time series standard deviation of the increments in surface and root zone soil moisture. This metric measures the typical magnitude of instantaneous increments. Typical increments in surface soil moisture are on the order of 0.02-0.03 m^3 m^{-3} in the central US, the Sahel, southern South America, southern Africa, India, portions of central Asia, and most of Australia. In the same regions, root zone soil moisture increments are typically on the order of 0.003-0.005s m^3 m^{-3}. Over densely vegetated regions, in particular the tropical forests, surface and root zone soil moisture increments are generally negligible, reflecting the fact that in those areas the measured SMAP brightness temperatures are mostly sensitive to the dense vegetation and are only marginally sensitive to soil moisture.

6.5.3 Uncertainty Estimates

The L4_SM data product also includes error estimates for key output variables, including surface and root zone soil moisture as well as surface soil temperature. These uncertainty estimates vary dynamically and geographically because they are computed as the standard deviation of a given output variable across the ensemble of land surface states at a given time and location. (The ensemble is an integral part of the ensemble Kalman filter employed in the L4_SM algorithm, and the ensemble average provides the estimate

of the variable under consideration (Reichle 2008).) By construction, the uncertainty estimates represent only the random component of the uncertainty. Bias and other structural errors such as errors in the dynamic range are not included.

Figure 18 shows the temporal mean of the uncertainty estimates for the validation period. Across the globe, surface soil moisture uncertainty typically ranges from 0.02 to 0.04 m^3 m^{-3} in Version 5, with larger uncertainties in regions where the lowest number of SMAP brightness temperatures are assimilated (Figure 12), including northwestern North America, northeastern Asia, and the Tibetan Plateau, which are subject to frozen or snow-covered conditions for a large part of the year. The less frequent brightness temperature analysis in these regions implies less reduction in ensemble spread. The uncertainty in root zone soil moisture exhibits a similar pattern, albeit with uncertainty estimates typically ranging from 0.01 to 0.02 m^3 m^{-3}. The lower uncertainty estimates in root zone soil moisture primarily reflect the fact that root zone soil moisture is less variable in time than surface soil moisture. The Version 5 uncertainty estimates are very close to those of Version 4 (Reichle et al. 2018b, their Figure 20).

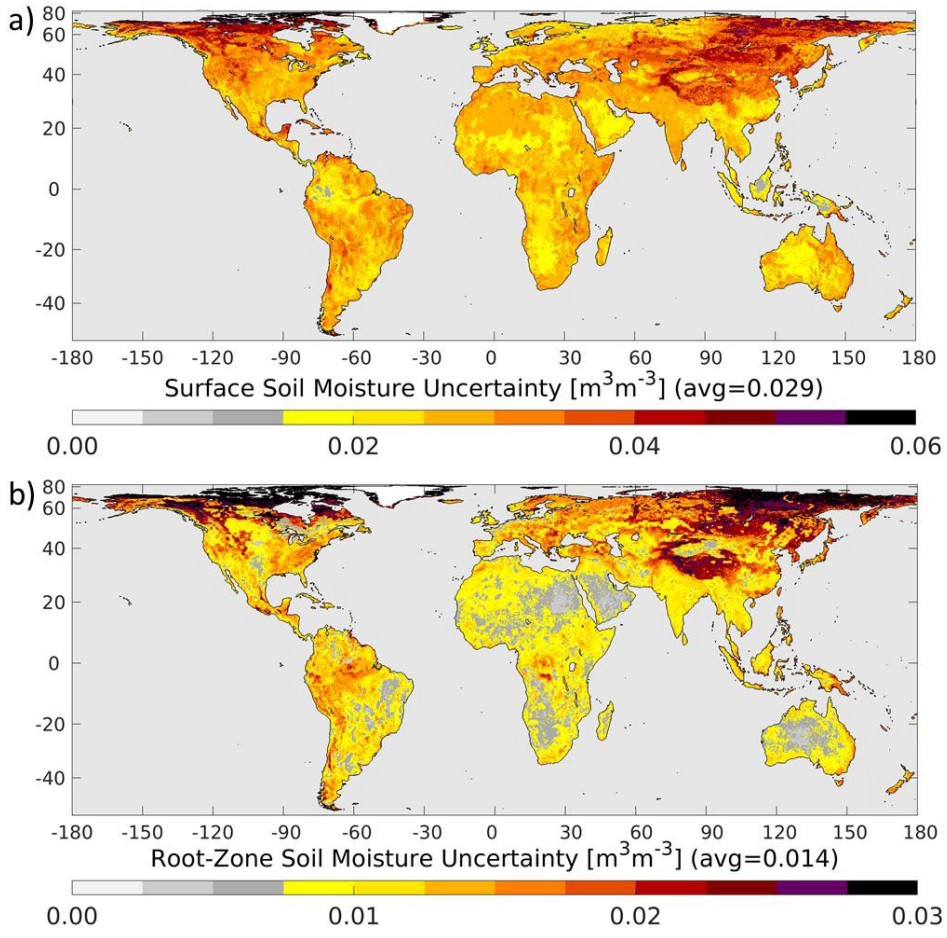

Figure 18. L4_SM (Vv5030) uncertainty estimates for (a) surface soil moisture and (b) root zone soil moisture averaged across the validation period (April 2015 – March 2021). Uncertainty estimates are computed as the standard deviation across the model ensemble that is used in the L4_SM assimilation algorithm. White shading indicates no-data-values.

7 LIMITATIONS AND PLAN FOR FUTURE IMPROVEMENTS

Several limitations and avenues for future development are revealed by the assessment of the Version 5 L4_SM product presented above and by Version 4 validation results (Reichle et al. 2018b, 2019, 2021) that still apply to Version 5.

7.1 L4_SM Algorithm Calibration and Temporal Homogeneity

Compared to earlier versions, the calibration of the Version 5 L4_SM algorithm utilized longer records of (i) model-only brightness temperature data and (ii) SMAP brightness temperature observations. Unlike in earlier versions, SMOS brightness temperature data were not used to derive the brightness temperature scaling parameters in Version 5. These changes improved the Version 5 algorithm calibration and further reduced the residual bias between the predicted brightness temperatures from the L4_SM modeling system and the (rescaled) SMAP observations, resulting in a less biased analysis than in Version 4. There are, however, still regions with a modest bias in the brightness temperature O-F residuals (Figure 13a), which in turn leads to non-zero long-term mean soil moisture analysis increments (Figure 16).

Eventually, further improvements in the L4_SM algorithm calibration will be facilitated by an even longer record of SMAP observations and matching model-only brightness temperature estimates. However, version changes in the GEOS FP system (Lucchesi, 2018) during the SMAP period adversely impact the homogeneity of the surface meteorological forcing data that are needed to calibrate the L4_SM algorithm and to generate the L4_SM data product. A forthcoming GEOS reanalysis product for the 21st century ("R21C") is expected to be available in 2023. This new reanalysis dataset will provide a more homogeneous record of surface meteorological forcing data during the SMAP period and will also be more consistent with the operational FP version that provides the surface meteorological forcing data for L4_SM forward processing. Once the R21C reanalysis is available, we plan to use the R21C data in future L4_SM versions for both calibration and L4_SM processing.

7.2 Impact of Ensemble Perturbations

Section 6.1 revealed that nonlinearities in the generation of the perturbations applied to the precipitation and shortwave forcing contribute to a small bias in L4_SM soil moisture when compared to the unperturbed model climatology. Now that the mechanism has been identified, it should be relatively straightforward to reduce this bias by relaxing the limit for outliers to a maximum of 3 times the standard deviation. Alternatively, approximate correction terms could perhaps be added into the ensemble perturbations scheme.

It is unclear, however, if anything can be done to reduce the wet soil moisture bias in arid regions that stems from the fact that at the dry end, soil moisture perturbations can only be positive (wetting). Reducing the standard deviation of the perturbations would reduce this bias, but it would also make the L4_SM algorithm insensitive to errors in the model forecast soil moisture (for lack of sufficient ensemble spread in the EnKF analysis).

7.3 Precipitation Data

Gauge-based precipitation data from the NOAA Climate Prediction Center Unified (CPCU) product provide an important contribution to the skill of the L4_SM soil moisture estimates (Reichle et al. 2021).

The same gauge-based precipitation data are also used in the MERRA-2 reanalysis (Gelaro et al., 2017; Reichle et al., 2017c). In both MERRA-2 and L4_SM, CPCU-based precipitation corrections are not applied in Africa and the high latitudes, owing to the sparsity of the precipitation gauge network there. Moreover, monitoring of the L4_SM O-F residuals and a verification of the L4_SM precipitation against independent observations revealed that the quality of the CPCU product is relatively poor in central Australia and in Myanmar (Reichle et al. 2017b, 2021). Finally, routine monitoring of the L4_SM and MERRA-2 data revealed a recent uptick in occurrences of erratic data values in the CPCU product in South America and Eurasia.

Ongoing L4_SM development efforts target the replacement of the CPCU inputs with satellite-based precipitation data from the NASA IMERG suite of products (Tan et al. 2019). IMERG, however, offers only data that are, at best, informed by monthly totals from precipitation gauges, and the gauge-corrected IMERG data have a latency of several months, which makes them suitable only for retrospective processing of L4_SM. Forward-processing would have to rely on satellite-only precipitation estimates. Preliminary results suggest that using IMERG instead of CPCU precipitation inputs improves the anomaly correlation skill of L4_SM soil moisture estimates in the Southern Hemisphere, including much of Africa and central Australia, even when just the satellite-only IMERG product is used.

7.4 L4_SM Algorithm Refinements

Recent research into improving the Catchment model parameterization for peat soils (Bechtold et al. 2019) and brightness temperature data assimilation in peatlands (Bechtold et al. 2020) provided encouraging results. Additional research suggests that relatively simple model revisions can improve the Catchment model skill in permafrost regions (Tao et al. 2017, 2019). Implementing these model advances in the L4_SM algorithm should improve the skill of the L4_SM product in the high latitudes, where the coupling with the carbon cycle is of particular interest in the context of the SMAP science objectives.

Research by the SMAP Level-2 (L2) soil moisture algorithm development team resulted in important advances in the skill of the retrievals from the dual-channel algorithm. This algorithm retrieves vegetation optical depth (VOD) along with surface soil moisture. This removes the dependency of the SMAP L2 retrievals on a pre-specified climatology of the normalized vegetation difference index (NDVI), which is based on optical data and from which VOD can only be determined approximately. Preliminary research by the L4_SM team is exploring the use of a climatology of L2-retrieved VOD in the L4_SM L-band brightness temperature radiative transfer model. While this would not change the use of climatological VOD information in the L4_SM algorithm, it would at least remove the dependency of the L4_SM algorithm on optical (NDVI) data to estimate VOD in the SMAP brightness temperature analysis.

8 SUMMARY AND CONCLUSIONS

This report provides an assessment of Version 5 of the SMAP L4_SM product. The validation covers the period from 1 April 2015, 0z to 1 April 2021, 0z. The Version 5 L4_SM algorithm was recalibrated to work with the substantially changed calibration of the assimilated Version 5 (R17) Level-1C brightness temperatures. The calibration of the L-band microwave radiative transfer model parameters was updated using a longer record of SMOS observations and the latest (NRv8.3) land model version. Moreover, longer records of SMAP observations and simulated brightness temperatures were used to improve the brightness temperature scaling parameters. Bug fixes in Version 5 address (i) an error in the Catchment model soil hydraulic parameters that potentially affected the simulation of soil moisture in about 2% of all land surface elements and (ii) an error in the perturbations of the photosynthetically active radiation that adversely impacted the model's water balance. Moreover, the Version 5 also includes minor changes in the Catchment model's surface turbulence calculations and major software infrastructure upgrades.

The Version 5 L4_SM product was validated using in situ soil moisture measurements from SMAP core validation sites and sparse networks. The product was further evaluated through an assessment of the data assimilation diagnostics generated by the L4_SM algorithm, such as the observation-minus-forecast residuals and the increments.

An analysis of the time-averaged surface and root zone soil moisture shows that the global pattern of arid and humid regions is captured by the Version 5 L4_SM estimates. Surface and root zone soil moisture is generally drier by 0.008 m^3 m^{-3} in Version 5 compared to Version 4. This climatological difference is caused by the complex interplay of the Version 5 system changes and bug fixes (section 6.1). Because of these climatological differences, the Version 4 and 5 products should *not* be combined into a single dataset for use in applications.

When compared to core validation site measurements, the Version 5 surface soil moisture ubRMSD is 0.040 m^3 m^{-3} at the 9 km scale and 0.037 m^3 m^{-3} at the 33 km scale. For root zone soil moisture, the ubRMSD is 0.027 m^3 m^{-3} at the 9 km scale and 0.024 m^3 m^{-3} at the 33 km scale. When factoring in the measurement error of the in situ measurements (conservatively estimated to be ~0.01-0.02 m^3 m^{-3}), the **Version 5 L4_SM surface and root zone soil moisture clearly meets the product accuracy requirement** (ubRMSE $\leq$ 0.04 m^3 m^{-3}). It is important to keep in mind that whereas the surface soil moisture in situ measurements are typically at ~5 cm depth, the L4_SM estimates are for the 0-5 cm soil layer. As with the error in the in situ measurements themselves, this mismatch in layer depths adversely impacts all given validation metrics.

The assimilation of SMAP brightness temperatures in the L4_SM algorithm is beneficial for surface and root zone soil moisture estimates, with improvements over the model-only open loop (OL5030) that are consistent across the 9 km and 33 km scales and across the ubRMSD and R metrics. For surface soil moisture, the correlation improvements are statistically significant (based on 95% confidence intervals). The comparison with in situ measurements from a global set of sparse networks corroborates the results obtained for the core validation sites.

The data assimilation diagnostics further broaden the validation to the global domain and indicate that the L4_SM system is nearly unbiased in the global average sense. The time mean, globally averaged analysis increments in surface and root zone soil moisture are very small. Regionally, however, time mean increments can be as large as 0.5 mm d^{-1}. These biases are caused by modest biases in the observation-minus-forecast residuals of brightness temperature in the L4_SM product that can be up to ±3 K in small regions. The assimilation diagnostics further reveal that, on a regional basis, the errors in brightness temperature are typically over- or underestimated considerably by the L4_SM system. However, the Version 5 assimilation diagnostics are generally improved over those of Version 4. The long-term mean absolute O-F brightness temperature residuals and soil moisture increments are reduced by 30-50% on

average. Moreover, the time series standard deviation of the O-F brightness temperature residuals is reduced from 5.7 K in Version 4 (3-year statistic) to 5.5 K in Version 5 (6-year statistic).

Uncertainty estimates for the analyzed surface soil moisture, root zone soil moisture, surface temperature, and top layer soil temperature are also provided with the product. These uncertainty estimates are designed to reflect the random error in key geophysical product fields. There are no relevant differences between the Version 4 and 5 uncertainty estimates.

Based on the results presented in this report, the public release of Version 5 of the L4_SM data product is recommended. The results, however, also uncovered limitations in the Version 5 product and possible avenues for future development, including the use of a forthcoming GEOS reanalysis that will provide a more temporally homogeneous record of surface meteorological forcing data (section 7.1), the use of IMERG precipitation products to replace the CPCU gauge-based inputs (section 7.2), the reduction of the nonlinear effects of the multiplicative ensemble perturbations to precipitation and shortwave forcing on the simulated soil moisture climatology (section 7.3), and the use of improved Catchment model physics for peatlands and permafrost (section 7.4). Moreover, calibration of the system with longer records should further reduce the residual regional bias in the observation-minus-forecast brightness temperature residuals and the resulting impact of non-zero long-term mean analysis increments on the water balance. Similarly, longer records of in situ measurements will permit more extensive validation. Additionally, the expected public availability of tower flux measurements for the SMAP period will support the evaluation of L4_SM latent and sensible heat flux estimates. These developments will be addressed in future work.

ACKNOWLEDGEMENTS

This report was made possible by the contributions of many individuals from the SMAP Project, the SMAP Science Team, the SMAP Cal/Val Partner Program, and the NASA Global Modeling and Assimilation Office. The NASA Soil Moisture Active Passive mission and the NASA Modeling, Analysis, and Prediction program supported the research. Computational resources were provided by the NASA High-End Computing Program through the NASA Center for Climate Simulation at the Goddard Space Flight Center.

APPENDIX

Performance Metrics at Core Validation Site Reference Pixels

Tables A1-A2 in this Appendix provide a complete listing of the performance metrics, including ubRMSD, MD, R, and anomaly R, for all 9 km and 33 km core site reference pixels. Metrics are provided for surface and root zone soil moisture for the L4_SM Vv5030 product and the model-only OL5030 estimates.

Table A1. Surface soil moisture metrics at individual reference pixels and averaged over 33 km and 9 km reference pixels, including average and average absolute MD (bottom rows labeled "All"). Information for 33 km reference pixels is shown in bold font. Italics indicate Version 5 L4_SM metrics. See Table 3 for full site names.

	Reference pixel		Surface soil moisture											
			ubRMSD (m3 m-3)			MD (m3 m-3)			R (dimensionless)			Anomaly R (dim.-less)		
Site name	ID	Horiz. scale (km)	OL5030	*Vv5030*	95% conf. interval	OL5030	*Vv5030*	95% conf. int.	OL5030	*Vv5030*	95% conf. interval	OL5030	*Vv5030*	95% conf. interval
RM	**03013302**	**33**	**0.028**	***0.037***	**0.005**	**0.043**	***0.046***	**0.007**	**0.82**	***0.82***	**0.05**	**0.69**	***0.75***	**0.05**
	03010903	9	0.029	*0.036*	0.004	0.127	*0.142*	0.005	0.62	*0.63*	0.08	0.61	*0.66*	0.08
	03010908	9	0.038	*0.047*	0.007	-0.015	*-0.013*	0.010	0.74	*0.70*	0.08	0.56	*0.60*	0.07
RC	**04013302**	**33**	**0.042**	***0.041***	**0.011**	**-0.010**	***-0.003***	**0.015**	**0.62**	***0.68***	**0.18**	**0.61**	***0.68***	**0.24**
	04010907	9	0.041	*0.041*	0.008	-0.027	*-0.023*	0.012	0.63	*0.67*	0.15	0.61	*0.71*	0.18
	04010910	9	0.048	*0.046*	0.014	-0.022	*-0.021*	0.018	0.70	*0.74*	0.14	0.52	*0.67*	0.17
YC	**07013301**	**33**	**0.045**	***0.036***	**0.008**	**-0.014**	***-0.022***	**0.011**	**0.87**	***0.90***	**0.04**	**0.82**	***0.90***	**0.04**
	07010902	9	0.075	*0.061*	0.014	-0.057	*-0.056*	0.019	0.84	*0.88*	0.05	0.73	*0.84*	0.06
	07010916	9	0.052	*0.045*	0.011	-0.010	*-0.019*	0.015	0.82	*0.86*	0.06	0.77	*0.85*	0.06
CR	**09013301**	**33**	**0.037**	***0.049***	**0.007**	**-0.021**	***-0.021***	**0.009**	**0.68**	***0.64***	**0.08**	**0.62**	***0.66***	**0.07**
	09010906	9	0.031	*0.048*	0.006	0.034	*0.034*	0.008	0.67	*0.68*	0.08	0.58	*0.70*	0.08
NG	**12033301**	**33**	**0.030**	***0.030***	**0.006**	**-0.017**	***-0.015***	**0.008**	**0.66**	***0.66***	**0.13**	**0.46**	***0.47***	**0.14**
WG	**16013302**	**33**	**0.026**	***0.029***	**0.002**	**0.024**	***0.031***	**0.003**	**0.74**	***0.80***	**0.05**	**0.70**	***0.78***	**0.05**
	16010906	9	0.027	*0.028*	0.002	-0.006	*0.005*	0.003	0.65	*0.72*	0.05	0.61	*0.70*	0.05
	16010907	9	0.028	*0.031*	0.002	0.021	*0.031*	0.003	0.66	*0.72*	0.05	0.61	*0.70*	0.05
	16010913	9	0.030	*0.037*	0.003	0.092	*0.094*	0.004	0.75	*0.81*	0.06	0.73	*0.81*	0.05
LW	**16023302**	**33**	**0.037**	***0.030***	**0.003**	**-0.043**	***-0.043***	**0.004**	**0.73**	***0.85***	**0.04**	**0.70**	***0.85***	**0.04**
	16020905	9	0.048	*0.042*	0.004	-0.005	*-0.001*	0.006	0.66	*0.75*	0.05	0.61	*0.72*	0.05
	16020906	9	0.043	*0.037*	0.004	-0.015	*-0.015*	0.005	0.68	*0.79*	0.05	0.66	*0.80*	0.04
	16020907	9	0.040	*0.034*	0.005	-0.046	*-0.047*	0.007	0.69	*0.81*	0.06	0.68	*0.79*	0.06
FC	**16033302**	**33**	**0.038**	***0.036***	**0.003**	**-0.034**	***-0.033***	**0.005**	**0.71**	***0.84***	**0.04**	**0.67**	***0.84***	**0.04**
	16030911	9	0.050	*0.040*	0.005	-0.056	*-0.052*	0.007	0.66	*0.81*	0.04	0.64	*0.83*	0.04
	16030916	9	0.037	*0.033*	0.003	-0.035	*-0.032*	0.004	0.70	*0.82*	0.04	0.70	*0.82*	0.03
LR	**16043302**	**33**	**0.041**	***0.040***	**0.003**	**0.002**	***0.002***	**0.004**	**0.70**	***0.74***	**0.05**	**0.67**	***0.72***	**0.05**
	16040901	9	0.033	*0.031*	0.003	0.074	*0.081*	0.004	0.79	*0.80*	0.05	0.77	*0.79*	0.04
SJ	**16063302**	**33**	**0.044**	***0.040***	**0.006**	**0.132**	***0.129***	**0.008**	**0.63**	***0.71***	**0.11**	**0.45**	***0.67***	**0.10**
	16060907	9	0.047	*0.041*	0.014	0.062	*0.056*	0.018	0.63	*0.72*	0.16	0.41	*0.66*	0.13
SF	**16073302**	**33**	**0.055**	***0.048***	**0.007**	**0.029**	***0.027***	**0.010**	**0.62**	***0.73***	**0.07**	**0.67**	***0.80***	**0.05**
	16070909	9	0.061	*0.054*	0.007	-0.012	*-0.013*	0.009	0.56	*0.68*	0.07	0.64	*0.78*	0.05
	16070910	9	0.062	*0.055*	0.007	0.033	*0.031*	0.009	0.53	*0.66*	0.08	0.59	*0.75*	0.06
	16070911	9	0.065	*0.057*	0.007	0.047	*0.045*	0.010	0.50	*0.63*	0.08	0.53	*0.70*	0.07
MB	**19023301**	**33**	**0.039**	***0.036***	**0.007**	**-0.068**	***-0.071***	**0.010**	**0.57**	***0.76***	**0.05**	**0.60**	***0.78***	**0.05**
	19020902	9	0.042	*0.036*	0.009	-0.060	*-0.071*	0.012	0.55	*0.79*	0.08	0.61	*0.81*	0.08
TZ	**25013301**	**33**	**0.039**	***0.034***	**0.011**	**0.012**	***0.014***	**0.015**	**0.92**	***0.94***	**0.04**	**0.67**	***0.73***	**0.07**
	25010911	9	0.042	*0.037*	0.010	0.006	*0.007*	0.014	0.90	*0.92*	0.05	0.64	*0.70*	0.07
KN	**27013301**	**33**	**0.042**	***0.038***	**0.008**	**0.020**	***0.019***	**0.011**	**0.58**	***0.72***	**0.09**	**0.64**	***0.74***	**0.07**
	27010910	9	0.032	*0.029*	0.006	-0.013	*-0.005*	0.008	0.62	*0.75*	0.09	0.65	*0.75*	0.08
	27010911	9	0.041	*0.036*	0.007	-0.040	*-0.037*	0.010	0.63	*0.76*	0.08	0.64	*0.73*	0.08
VA	41010906	9	0.029	*0.027*	0.006	0.066	*0.066*	0.009	0.55	*0.65*	0.18	0.65	*0.73*	0.17
NI	**45013301**	**33**	**0.041**	***0.038***	**0.006**	**0.036**	***0.058***	**0.009**	**0.32**	***0.55***	**0.21**	n/a	n/a	n/a
	45010902	9	0.041	*0.039*	0.005	0.045	*0.067*	0.007	0.25	*0.48*	0.18	0.16	*0.44*	0.15
BN	**45023301**	**33**	**0.051**	***0.047***	**0.009**	**0.126**	***0.128***	**0.013**	**0.68**	***0.73***	**0.11**	**0.32**	***0.47***	**0.13**
	45020902	9	0.051	*0.047*	0.010	0.124	*0.127*	0.013	0.74	*0.78*	0.10	0.32	*0.47*	0.13
TX	**48013301**	**33**	**0.034**	***0.028***	**0.004**	**0.032**	***0.030***	**0.006**	**0.83**	***0.91***	**0.04**	**0.78**	***0.88***	**0.04**
	48010902	9	0.039	*0.036*	0.004	0.068	*0.067*	0.006	0.74	*0.83*	0.05	0.67	*0.79*	0.05
	48010911	9	0.038	*0.032*	0.004	0.077	*0.076*	0.006	0.79	*0.87*	0.05	0.72	*0.84*	0.05
HB	**67013301**	**33**	**0.034**	***0.031***	**0.008**	**-0.012**	***-0.014***	**0.010**	**0.78**	***0.82***	**0.05**	**0.68**	***0.77***	**0.05**
	67010901	9	0.045	*0.045*	0.021	-0.015	*-0.013*	0.026	0.83	*0.83*	0.10	0.46	*0.63*	0.17
All	**Average**	**33**	**0.039**	***0.037***	**0.002**	**0.013**	***0.015***	**0.002**	**0.69**	***0.77***	**0.02**	**0.63**	***0.73***	**0.02**
	Average	9	0.042	*0.040*	0.002	0.021	*0.023*	0.002	0.67	*0.75*	0.02	0.58	*0.71*	0.02
	Avg. Abs.	**33**	Same as average.			**0.037**	***0.039***	**0.002**	Same as average.					
	Avg. Abs.	9				0.047	*0.049*	0.002						

Table A2. As in Table A1 but for root zone soil moisture.

Site name	Reference pixel		Root zone soil moisture											
			ubRMSD (m3 m-3)			MD (m3 m-3)			R (dimensionless)			Anomaly R (dim.-less)		
	ID	Horiz. scale (km)	OL5030	*Vv5030*	95% conf. interval	OL5030	*Vv5030*	95% conf. interval	OL5030	*Vv5030*	95% conf. interval	OL5030	*Vv5030*	95% conf. interval
RM	**03013302**	**33**	n/a	n/a	n/a	n/a	n/a	n/a	n/a	n/a	n/a	n/a	n/a	n/a
	03010903	9	n/a	n/a	n/a	n/a	n/a	n/a	n/a	n/a	n/a	n/a	n/a	n/a
	03010908	9	n/a	n/a	n/a	n/a	n/a	n/a	n/a	n/a	n/a	n/a	n/a	n/a
RC	**04013302**	**33**	n/a	n/a	n/a	n/a	n/a	n/a	n/a	n/a	n/a	n/a	n/a	n/a
	04010907	9	n/a	n/a	n/a	n/a	n/a	n/a	n/a	n/a	n/a	n/a	n/a	n/a
	04010910	9	n/a	n/a	n/a	n/a	n/a	n/a	n/a	n/a	n/a	n/a	n/a	n/a
YC	**07013301**	**33**	**0.010**	***0.007***	**0.006**	**-0.111**	***-0.100***	**0.007**	**0.90**	***0.96***	**0.21**	**n/a**	***n/a***	**n/a**
	07010902	9	n/a	n/a	n/a	n/a	n/a	n/a	n/a	n/a	n/a	n/a	n/a	n/a
	07010916	9	n/a	n/a	n/a	n/a	n/a	n/a	n/a	n/a	n/a	n/a	n/a	n/a
CR	**09013301**	**33**	n/a	n/a	n/a	n/a	n/a	n/a	n/a	n/a	n/a	n/a	n/a	n/a
	09010906	9	n/a	n/a	n/a	n/a	n/a	n/a	n/a	n/a	n/a	n/a	n/a	n/a
NG	**12033301**	**33**	n/a	n/a	n/a	n/a	n/a	n/a	n/a	n/a	n/a	n/a	n/a	n/a
WG	**16013302**	**33**	n/a	n/a	n/a	n/a	n/a	n/a	n/a	n/a	n/a	n/a	n/a	n/a
	16010906	9	n/a	n/a	n/a	n/a	n/a	n/a	n/a	n/a	n/a	n/a	n/a	n/a
	16010907	9	n/a	n/a	n/a	n/a	n/a	n/a	n/a	n/a	n/a	n/a	n/a	n/a
	16010913	9	n/a	n/a	n/a	n/a	n/a	n/a	n/a	n/a	n/a	n/a	n/a	n/a
LW	**16023302**	**33**	**0.030**	***0.027***	**0.004**	**-0.035**	***-0.034***	**0.006**	**0.73**	***0.80***	**0.10**	**0.68**	***0.82***	**0.09**
	16020905	9	n/a	n/a	n/a	n/a	n/a	n/a	n/a	n/a	n/a	n/a	n/a	n/a
	16020906	9	0.030	*0.026*	0.004	-0.010	*-0.010*	0.006	0.64	*0.74*	0.13	0.60	*0.75*	0.12
	16020907	9	0.034	*0.031*	0.008	-0.032	*-0.033*	0.011	0.70	*0.78*	0.14	n/a	n/a	n/a
FC	**16033302**	**33**	**0.029**	***0.023***	**0.004**	**0.027**	***0.039***	**0.005**	**0.71**	***0.82***	**0.11**	**0.66**	***0.81***	**0.11**
	16030911	9	0.034	*0.028*	0.005	-0.012	*0.001*	0.007	0.70	*0.82*	0.11	0.64	*0.81*	0.10
	16030916	9	0.025	*0.023*	0.003	-0.012	*-0.002*	0.005	0.70	*0.78*	0.10	0.62	*0.76*	0.09
LR	**16043302**	**33**	**0.030**	***0.029***	**0.003**	**0.066**	***0.066***	**0.004**	**0.65**	***0.66***	**0.12**	**0.60**	***0.63***	**0.11**
	16040901	9	0.027	*0.027*	0.003	0.093	*0.097*	0.005	0.61	*0.60*	0.15	0.66	*0.65*	0.13
SJ	**16063302**	**33**	n/a	n/a	n/a	n/a	n/a	n/a	n/a	n/a	n/a	n/a	n/a	n/a
	16060907	9	n/a	n/a	n/a	n/a	n/a	n/a	n/a	n/a	n/a	n/a	n/a	n/a
SF	**16073302**	**33**	**0.034**	***0.035***	**0.006**	**0.010**	***0.010***	**0.008**	**0.62**	***0.61***	**0.19**	**0.75**	***0.87***	**0.11**
	16070909	9	0.038	*0.038*	0.006	-0.045	*-0.045*	0.008	0.56	*0.58*	0.18	0.72	*0.86*	0.10
	16070910	9	0.038	*0.038*	0.005	0.032	*0.032*	0.007	0.42	*0.44*	0.20	0.61	*0.83*	0.11
	16070911	9	0.037	*0.036*	0.005	0.024	*0.023*	0.007	0.44	*0.44*	0.19	0.57	*0.78*	0.12
MB	**19023301**	**33**	n/a	n/a	n/a	n/a	n/a	n/a	n/a	n/a	n/a	n/a	n/a	n/a
	19020902	9	n/a	n/a	n/a	n/a	n/a	n/a	n/a	n/a	n/a	n/a	n/a	n/a
TZ	**25013301**	**33**	**0.026**	***0.028***	**0.015**	**0.032**	***0.032***	**0.018**	**0.93**	***0.92***	**0.11**	**0.79**	***0.79***	**0.18**
	25010911	9	0.027	*0.029*	0.013	0.032	*0.033*	0.016	0.92	*0.90*	0.13	0.79	*0.80*	0.16
KN	**27013301**	**33**	**0.025**	***0.021***	**0.013**	**-0.017**	***-0.015***	**0.015**	**0.79**	***0.85***	**0.24**	**0.84**	***0.89***	**0.17**
	27010910	9	n/a	n/a	n/a	n/a	n/a	n/a	n/a	n/a	n/a	n/a	n/a	n/a
	27010911	9	0.027	*0.022*	0.008	-0.039	*-0.034*	0.011	0.82	*0.88*	0.15	0.82	*0.89*	0.12
VA	41010906	9	n/a	n/a	n/a	n/a	n/a	n/a	n/a	n/a	n/a	n/a	n/a	n/a
NI	**45013301**	**33**	n/a	n/a	n/a	n/a	n/a	n/a	n/a	n/a	n/a	n/a	n/a	n/a
	45010902	9	n/a	n/a	n/a	n/a	n/a	n/a	n/a	n/a	n/a	n/a	n/a	n/a
BN	**45023301**	**33**	n/a	n/a	n/a	n/a	n/a	n/a	n/a	n/a	n/a	n/a	n/a	n/a
	45020902	9	n/a	n/a	n/a	n/a	n/a	n/a	n/a	n/a	n/a	n/a	n/a	n/a
TX	**48013301**	**33**	**0.023**	***0.020***	**0.006**	**0.047**	***0.049***	**0.008**	**0.91**	***0.94***	**0.08**	**0.89**	***0.93***	**0.08**
	48010902	9	0.026	*0.022*	0.005	0.111	*0.112*	0.007	0.79	*0.85*	0.13	0.72	*0.81*	0.13
	48010911	9	0.020	*0.017*	0.004	0.107	*0.109*	0.006	0.90	*0.93*	0.08	0.88	*0.93*	0.07
HB	**67013301**	**33**	n/a	n/a	n/a	n/a	n/a	n/a	n/a	n/a	n/a	n/a	n/a	n/a
	67010901	9	n/a	n/a	n/a	n/a	n/a	n/a	n/a	n/a	n/a	n/a	n/a	n/a
All	**Average**	**33**	**0.026**	***0.024***	**0.002**	**0.002**	***0.006***	**0.003**	**0.78**	***0.82***	**0.05**	**0.74**	***0.82***	**0.05**
	Average	9	0.029	*0.027*	0.002	0.024	*0.027*	0.003	0.72	*0.76*	0.05	0.70	*0.80*	0.05
	Avg. Abs.	**33**	Same as average.			**0.043**	***0.043***	**0.003**	Same as average.					
	Avg. Abs.	9				0.049	*0.047*	0.003						

REFERENCES

Bechtold, M., G. J. M. De Lannoy, R. D. Koster, R. H. Reichle, S. P. Mahanama, et al. (2019), PEAT-CLSM: A Specific Treatment of Peatland Hydrology in the NASA Catchment Land Surface Model, *Journal of Advances in Modeling Earth Systems, 11*, 2130-2162, doi:10.1029/2018MS001574.

Bechtold, M., G. J. M. De Lannoy, R. H. Reichle, D. Roose, N. Balliston, I. Burdun, K. Devito, J. Kurbatova, M. Strack, and E. A. Zarov (2020), Improved Groundwater Table and L-band Brightness Temperature Estimates for Northern Hemisphere Peatlands Using New Model Physics and SMOS Observations in a Global Data Assimilation Framework, *Remote Sensing of Environment, 246*, 111805, doi:10.1016/j.rse.2020.111805.

Bell, J. E., Palecki, M. A., Baker, C. B., Collins, W. G., Lawrimore, J. H., Leeper, R. D., Hall, M. E., Kochendorfer, J., Meyers, T. P., Wilson, T., & Diamond, H. J. (2013), U.S. Climate Reference Network soil moisture and temperature observations, *Journal of Hydrometeorology, 14*, 977–988, doi:10.1175/jhm-d-12-0146.1.

Bircher, S., N. Skou, K. H. Jensen, J. P. Walker, and L. Rasmussen (2012), A soil moisture and temperature network for SMOS validation in Western Denmark, *Hydrology and Earth System Sciences, 16*, 1445–1463, doi:10.5194/hess-16-1445-2012.

Bosch, D. D., J. M. Sheridan, and L. K. Marshall (2007), Precipitation, soil moisture, and climate database, Little River Experimental Watershed, Georgia, United States, *Water Resources Research*, 43, doi:10.1029/2006wr005834.

Caldwell, T. G., T. Bongiovanni, M. H. Cosh, C. Halley, and M. H. Young (2018), Field and Laboratory Evaluation of the CS655 Soil Water Content Sensor, *Vadose Zone Journal, 17*, 170214, doi:10.2136/vzj2017.12.0214.

Calvet, J.-C., N. Fritz, F. Froissard, D. Suquia, A. Petitpa, and B. Piguet (2007), In situ soil moisture observations for the CAL/VAL of SMOS: the SMOSMANIA network, 2007 IEEE International Geoscience and Remote Sensing Symposium, doi:10.1109/igarss.2007.4423019.

CEOS (2015), Committee on Earth Observation Satellites (CEOS) Working Group on Calibration and Validation (WGCV): http://calvalportal.ceos.org, CEOS WGCV Land Products Sub-Group: http://lpvs.gsfc.nasa.gov. Accessed 7 October 2015.

Chan, S., E. G. Njoku, and A. Colliander (2020), *SMAP L1C Radiometer Half-Orbit 36 km EASE-Grid Brightness Temperatures, Version 5*. NASA National Snow and Ice Data Center Distributed Active Archive Center, doi:10.5067/JJ5FL7FRLKJI.

Chen, F., W. T. Crow, A. Colliander, M. Cosh, T. J. Jackson, R. Bindlish, R. H. Reichle, S. K. Chan, D. D. Bosch, P. J. Starks, D. C. Goodrich, M. Seyfried (2016), Application of Triple Collocation in Ground-based Validation of Soil Moisture Active/Passive (SMAP) Level 2 Data Products, *IEEE Journal of Selected Topics in Applied Earth Observations and Remote Sensing*, submitted.

Chen, F. et al. (2019), Uncertainty of Reference Pixel Soil Moisture Averages Sampled at SMAP Core Validation Sites, *Journal of Hydrometeorology, 20,* 1553–1569, doi:10.1175/jhm-d-19-0049.1.

Clewley, D., J. B. Whitcomb, R. Akbar, A. R. Silva, A. Berg, J. R. Adams, T. Caldwell, D. Entekhabi, and M. Moghaddam (2017), A Method for Upscaling In Situ Soil Moisture Measurements to Satellite Footprint Scale Using Random Forests, *IEEE Journal of Selected Topics in Applied Earth Observations and Remote Sensing*, 10(6), 2663–2673, doi:10.1109/jstars.2017.2690220.

Colliander, A., S. Chan, N. Das, S. Kim, S. Dunbar, T. Jackson, C. Derksen, K. McDonald, J. Kimball, E. Njoku, R. Reichle, and B. Weiss (2014), SMAP L2-L4 Data Products Calibration and Validation Plan, Soil Moisture Active Passive (SMAP) Mission Science Document. JPL D-79463, Jet Propulsion Laboratory, Pasadena, CA.

Colliander, A., et al. (2017a), SMAP/In Situ Core Validation Site Land Surface Parameters Match-Up Data, Version 1. NASA National Snow and Ice Data Center DAAC, doi:10.5067/DXAVIXLY18KM.

Colliander, A. et al. (2017b), Validation of SMAP surface soil moisture products with core validation sites, *Remote Sensing of Environment, 191*, 215–231, doi:10.1016/j.rse.2017.01.021.

Colliander, A., R. H. Reichle, W. T. Crow, M. H. Cosh, et al. (2021), Validation of Soil Moisture Data Products from the NASA SMAP Mission, *IEEE Journal of Selected Topics in Applied Earth Observations and Remote Sensing*, submitted. Preprint available at http://doi.org/10.36227/techrxiv.14714571.

Coopersmith, E. J., M. H. Cosh, W. A. Petersen, J. Prueger, and J. J. Niemeier (2015), Soil Moisture Model Calibration and Validation: An ARS Watershed on the South Fork Iowa River, *Journal of Hydrometeorology, 16*, 1087–1101, doi:10.1175/jhm-d-14-0145.1.

Cosh, M. H., T. J. Jackson, P. Starks, and G. Heathman (2006), Temporal stability of surface soil moisture in the Little Washita River watershed and its applications in satellite soil moisture product validation, *Journal of Hydrology, 323*, 168–177, doi:10.1016/j.jhydrol.2005.08.020.

Cosh, M. H., P. J. Starks, J. A. Guzman, and D. N. Moriasi (2014), Upper Washita River Experimental Watersheds: Multiyear Stability of Soil Water Content Profiles, *Journal of Environmental Quality, 43*, 1328–1333, doi:10.2134/jeq2013.08.0318.

De Lannoy, G. J. M, R. H. Reichle, and V. R. N. Pauwels (2013), Global Calibration of the GEOS-5 L-band Microwave Radiative Transfer Model over Nonfrozen Land Using SMOS Observations, *Journal of Hydrometeorology, 14*, 765-785, doi:10.1175/JHM-D-12-092.1.

De Lannoy, G. J. M., R. H. Reichle, and J. A. Vrugt (2014a), Uncertainty Quantification of GEOS-5 L-Band Radiative Transfer Model Parameters using Bayesian Inference and SMOS Observations, *Remote Sensing of Environment, 148*, 146-157, doi:10.1016/j.rse.2014.03.030.

De Lannoy, G. J. M., R. D. Koster, R. H. Reichle, S. P. P. Mahanama, and Q. Liu (2014b), An Updated Treatment of Soil Texture and Associated Hydraulic Properties in a Global Land Modeling System, *Journal of Advances in Modeling Earth Systems, 6*, 957-979, doi:10.1002/2014MS000330.

De Lannoy, G. J. M., and R. H. Reichle (2016), Global Assimilation of Multiangle and Multipolarization SMOS Brightness Temperature Observations into the GEOS-5 Catchment Land Surface Model for Soil Moisture Estimation, *Journal of Hydrometeorology, 17*, 669-691, doi:10.1175/JHM-D-15-0037.1.

Diamond, H. J. et al. (2013), U.S. Climate Reference Network after One Decade of Operations: Status and Assessment, *Bulletin of the American Meteorological Society, 94*, 485–498, doi:10.1175/bams-d-12-00170.1.

Dong, J., W. T. Crow, K. J. Tobin, M. H. Cosh, D. D. Bosch, P. J. Starks, M. Seyfried, and C. Holifield-Collins (2020), Comparison of microwave remote sensing and land surface modeling for surface soil moisture climatology estimation, *Remote Sensing of Environment*, *242*, 111756, doi:10.1016/j.rse.2020.111756.

Entekhabi, D., R. H. Reichle, R. D. Koster, and W. T. Crow (2010), Performance Metrics for Soil Moisture Retrievals and Application Requirements, *Journal of Hydrometeorology, 11*, 832-840, doi:10.1175/2010JHM1223.1.

Entekhabi, D., et al. (2014), SMAP Handbook, *JPL Publication, JPL 400-1567*, NASA Jet Propulsion Laboratory, Pasadena, California, USA, 182 pp.

Galle, S. et al. (2018), AMMA-CATCH, a Critical Zone Observatory in West Africa Monitoring a Region in Transition, *Vadose Zone Journal*, 17(1), 0, doi:10.2136/vzj2018.03.0062.

Gelaro, R., et al. (2017), The Modern-Era Retrospective Analysis for Research and Applications, Version-2 (MERRA-2), *Journal of Climate, 30*, 5419-5454, doi:10.1175/JCLI-D-16-0758.1.

González-Zamora, Á., N. Sánchez, J. Martínez-Fernández, Á. Gumuzzio, M. Piles, and E. Olmedo (2015), Long-term SMOS soil moisture products: A comprehensive evaluation across scales and methods in the Duero Basin (Spain), *Physics and Chemistry of the Earth, Parts A/B/C*, 83-84, 123–136, doi:10.1016/j.pce.2015.05.009.

Gruber, A., C.-H. Su, S. Zwieback, W. Crow, W. Dorigo, and W. Wagner (2016), Recent advances in (soil moisture) triple collocation analysis, *International Journal of Applied Earth Observation and Geoinformation*, *45B*, 200-211, doi: 10.1016/j.jag.2015.09.002.

Gruber, A., et al. (2020), Validation practices for satellite soil moisture retrievals: What are (the) errors?, *Remote Sensing of Environment, 244*, 111806, doi:10.1016/j.rse.2020.111806.

Heathman, G. C., M. H. Cosh, V. Merwade, and E. Han (2012), Multi-scale temporal stability analysis of surface and subsurface soil moisture within the Upper Cedar Creek Watershed, Indiana, *CATENA*, 95, 91–103, doi:10.1016/j.catena.2012.03.008.

Helfand, H. M., and Schubert, S. D. (1995), Climatology of the Simulated Great Plains Low-Level Jet and Its Contribution to the Continental Moisture Budget of the United States, *Journal of Climate, 8*, 784-806, doi:10.1175/1520-0442(1995)008<0784:cotsgp>2.0.co;2.

Jackson, T. J., A. Colliander, J. Kimball, R. Reichle, C. Derksen, W. Crow, D. Entekhabi, P. O'Neill, and E. Njoku (2014), SMAP Science Data Calibration and Validation Plan (Revision A), Soil Moisture Active Passive (SMAP) Mission Science Document. JPL D-52544, Jet Propulsion Laboratory, Pasadena, CA.

Jensen, K. H., and J. C. Refsgaard (2018), HOBE: The Danish Hydrological Observatory, *Vadose Zone Journal, 17*, 180059, doi:10.2136/vzj2018.03.0059.

Juglea, S., Y. Kerr, A. Mialon, J.-P. Wigneron, E. Lopez-Baeza, A. Cano, A. Albitar, C. Millan-Scheiding, M. Carmen Antolin, and S. Delwart (2010), Modelling soil moisture at SMOS scale by use of a SVAT model over the Valencia Anchor Station, *Hydrology and Earth System Sciences*, 14(5), 831–846, doi:10.5194/hess-14-831-2010.

Keefer, T. O., M. S. Moran, and G. B. Paige (2008), Long-term meteorological and soil hydrology database, Walnut Gulch Experimental Watershed, Arizona, United States, *Water Resources Research, 44*, doi:10.1029/2006wr005702.

Khodayar, S., A. Coll, and E. Lopez-Baeza (2019), An improved perspective in the spatial representation of soil moisture: potential added value of SMOS disaggregated 1-km resolution "all weather" product, *Hydrology and Earth System Sciences*, 23(1), 255–275, doi:10.5194/hess-23-255-2019.

Koster, R. D., M. J. Suarez, A. Ducharne, M. Stieglitz, and P. Kumar (2000), A catchment-based approach to modeling land surface processes in a general circulation model: 1. Model structure, *J. Geophys. Res., 105*, 24809–24822, doi:10.1029/2000JD900327.

Koster, R. D., R. H. Reichle, S. P. P. Mahanama, J. Perket, Q. Liu, and G. Partyka (2020), Land-Focused Changes in the Updated GEOS FP System (Version 5.25), NASA Global Modeling and Assimilation Office Research Brief, 11pp. Available at: https://gmao.gsfc.nasa.gov/researchbriefs/land_changes_GEOS-FP/land_changes_GEOS-FP.pdf.

Liu, Q., R. H. Reichle, R. Bindlish, M. H. Cosh, W. T. Crow, R. de Jeu, G. J. M. De Lannoy, G. J. Huffman, and T. J. Jackson (2011), The contributions of precipitation and soil moisture observations to the skill of soil moisture estimates in a land data assimilation system, *Journal of Hydrometeorology, 12*, 750-765, doi:10.1175/JHM-D-10-05000.1.

Louis, J.-F. (1979), A parametric model of vertical eddy fluxes in the atmosphere, *Boundary-Layer Meteorology, 17*, 187-202, doi:10.1007/bf00117978.

Lucchesi, R. (2018), File specification for GEOS-5 FP, *NASA GMAO Office Note No. 4 (version 1.2)*, 56 pp., NASA Goddard Space Flight Center, Greenbelt, MD, USA. Available at: https://gmao.gsfc.nasa.gov/pubs

McNairn, H. et al. (2015), The Soil Moisture Active Passive Validation Experiment 2012 (SMAPVEX12): Prelaunch Calibration and Validation of the SMAP Soil Moisture Algorithms, *IEEE Transactions on Geoscience and Remote Sensing, 53*, 2784–2801, doi:10.1109/tgrs.2014.2364913.

McPherson, R. A. et al. (2007), Statewide Monitoring of the Mesoscale Environment: A Technical Update on the Oklahoma Mesonet, *Journal of Atmospheric and Oceanic Technology, 24*, 301–321, doi:10.1175/jtech1976.1.

Moghaddam, M. et al. (2016), *Soil Moisture Profiles and Temperature Data from SoilSCAPE Sites, USA*, ORNL Distributed Active Archive Center, doi:10.3334/ornldaac/1339.

Montzka, C., et al. (2020), Soil Moisture Product Validation Good Practices Protocol Version 1.0., In: *Good Practices for Satellite Derived Land Product Validation, Land Product Validation Subgroup*

(WGCV/CEOS), edited by C. Montzka, M. Cosh, J. Nickeson, F. Camacho, 123 pp, doi:10.5067/doc/ceoswgcv/lpv/sm.001.

Panciera, R., et al. (2014), The Soil Moisture Active Passive Experiments (SMAPEx): Toward Soil Moisture Retrieval From the SMAP Mission, *IEEE Transactions on Geoscience and Remote Sensing, 52*, 490–507, doi:10.1109/tgrs.2013.2241774.

Peng, J., et al. (2020), SMAP Radiometer Brightness Temperature Calibration for the L1B_TB (Version 5), L1C_TB (Version 5), and L1C_TB_E (Version 3) Data Products, SMAP Project, JPL-D 56295, Jet Propulsion Laboratory, Pasadena, CA. Available at: https://nsidc.org/data/smap/data_versions.

Reichle, R. H. (2008), Data Assimilation Methods in the Earth Sciences, *Advances in Water Resources, 31*, 1411-1418, doi:10.1016/j.advwatres.2008.01.001.

Reichle, R. H., and Q. Liu (2014), Observation-Corrected Precipitation Estimates in GEOS-5, *NASA Technical Report Series on Global Modeling and Data Assimilation, NASA/TM-2014-104606, Vol. 35*, National Aeronautics and Space Administration, Goddard Space Flight Center, Greenbelt, Maryland, USA, 18pp. Available at: https://gmao.gsfc.nasa.gov/pubs.

Reichle, R. H., G. J. M. De Lannoy, B. A. Forman, C. S. Draper, and Q. Liu (2014a), Connecting Satellite Observations with Water Cycle Variables through Land Data Assimilation: Examples Using the NASA GEOS-5 LDAS, *Surveys in Geophysics, 35*, 577-606, doi:10.1007/s10712-013-9220-8.

Reichle, R. H., R. Koster, G. De Lannoy, W. Crow, and J. Kimball (2014b), SMAP Level 4 Surface and Root Zone Soil Moisture Data Product: L4_SM Algorithm Theoretical Basis Document (Revision A), Soil Moisture Active Passive (SMAP) Mission Science Document. JPL D-66483, Jet Propulsion Laboratory, Pasadena, CA.

Reichle, R. H., G. J. M. De Lannoy, Q. Liu, A. Colliander, A. Conaty, T. Jackson, J. Kimball, and R. D. Koster (2015), Soil Moisture Active Passive (SMAP) Project Assessment Report for the Beta-Release L4_SM Data Product, *NASA Technical Report Series on Global Modeling and Data Assimilation, NASA/TM-2015-104606, Vol. 40*, National Aeronautics and Space Administration, Goddard Space Flight Center, Greenbelt, Maryland, USA, 63pp. Available at: https://gmao.gsfc.nasa.gov/pubs.

Reichle, R. H., G. J. M. De Lannoy, Q. Liu, J. V. Ardizzone, F. Chen, A. Colliander, A. Conaty, W. Crow, T. Jackson, J. Kimball, R. D. Koster, and E. B. Smith (2016), Soil Moisture Active Passive Mission L4_SM Data Product Assessment (Version 2 Validated Release), *NASA GMAO Office Note No. 12 (Version 1.0)*, 55pp., NASA Goddard Space Flight Center, Greenbelt, MD, USA. Available at: https://gmao.gsfc.nasa.gov/pubs

Reichle, R. H., et al. (2017a), Assessment of the SMAP Level-4 Surface and Root-Zone Soil Moisture Product Using In Situ Measurements, *Journal of Hydrometeorology, 18*, 2621-2645, doi:10.1175/JHM-D-17-0063.1.

Reichle, R. H., et al. (2017b), Global Assessment of the SMAP Level-4 Surface and Root-Zone Soil Moisture Product Using Assimilation Diagnostics, *Journal of Hydrometeorology, 18*, 3217-3237, doi:10.1175/JHM-D-17-0130.1.

Reichle, R. H., Q. Liu, R. D. Koster, C. S. Draper, S. P. P. Mahanama, and G. S. Partyka (2017c), Land surface precipitation in MERRA-2, *Journal of Climate, 30*, 1643-1664, doi:10.1175/JCLI-D-16-0570.1.

Reichle, R. H., R. A. Lucchesi, J. V. Ardizzone, G.-K. Kim, E. B. Smith, and B. H. Weiss (2018a), Soil Moisture Active Passive (SMAP) Mission Level 4 Surface and Root Zone Soil Moisture (L4_SM) Product Specification Document, *NASA GMAO Office Note No. 10 (Version 1.5)*, 83 pp., NASA Goddard Space Flight Center, Greenbelt, MD, USA. Available at: https://gmao.gsfc.nasa.gov/pubs.

Reichle, R. H., Q. Liu, R. D. Koster, J. V. Ardizzone, A. Colliander, W. T. Crow, G. J. M. De Lannoy, and J. S. Kimball (2018b), Soil Moisture Active Passive (SMAP) Project Assessment Report for Version 4 of the L4_SM Data Product, *NASA Technical Report Series on Global Modeling and Data Assimilation, NASA/TM-2018-104606, Vol. 52*, National Aeronautics and Space Administration, Goddard Space Flight Center, Greenbelt, Maryland, USA, 72pp. Available at: https://gmao.gsfc.nasa.gov/pubs.

Reichle, R., G. De Lannoy, R. D. Koster, W. T. Crow, J. S. Kimball, and Q. Liu (2018c), *SMAP L4 9 km EASE-Grid Surface and Root Zone Soil Moisture Analysis Update, Version 4*. NASA National Snow and Ice Data Center Distributed Active Archive Center, doi:10.5067/60HB8VIP2T8W.

Reichle, R., G. De Lannoy, R. D. Koster, W. T. Crow, J. S. Kimball, and Q. Liu (2018d), *SMAP L4 9 km EASE-Grid Surface and Root Zone Soil Moisture Geophysical Data, Version 4*. NASA National Snow and Ice Data Center Distributed Active Archive Center, doi:10.5067/KPJNN2GI1DQR.

Reichle, R., G. De Lannoy, R. D. Koster, W. T. Crow, J. S. Kimball, and Q. Liu (2018e), *SMAP L4 9 km EASE-Grid Surface and Root Zone Soil Moisture Land Model Constants, Version 4*. NASA National Snow and Ice Data Center Distributed Active Archive Center, doi:10.5067/KGLC3UH4TMAQ.

Reichle, R. H., et al. (2019), Version 4 of the SMAP Level-4 Soil Moisture Algorithm and Data Product, *Journal of Advances in Modeling Earth Systems, 11*, 3106-3130, doi:10.1029/2019MS001729.

Reichle, R., G. De Lannoy, R. D. Koster, W. T. Crow, J. S. Kimball, and Q. Liu (2020a), *SMAP L4 Global 3-hourly 9 km EASE-Grid Surface and Root Zone Soil Moisture Analysis Update, Version 5*. NASA National Snow and Ice Data Center Distributed Active Archive Center, doi:10.5067/0D8JT6S27BS9.

Reichle, R., G. De Lannoy, R. D. Koster, W. T. Crow, J. S. Kimball, and Q. Liu (2020b), *SMAP L4 Global 3-hourly 9 km EASE-Grid Surface and Root Zone Soil Moisture Geophysical Data, Version 5*. NASA National Snow and Ice Data Center Distributed Active Archive Center, doi:10.5067/9LNYIYOBNBR5.

Reichle, R., G. De Lannoy, R. D. Koster, W. T. Crow, J. S. Kimball, and Q. Liu (2020c), *SMAP L4 Global 3-hourly 9 km EASE-Grid Surface and Root Zone Soil Moisture Land Model Constants, Version 5*. NASA National Snow and Ice Data Center Distributed Active Archive Center, doi:10.5067/5C36BVQZW28K.

Reichle, R. H., et al. (2021), The Contributions of Gauge-Based Precipitation and SMAP Brightness Temperature Observations to the Skill of the SMAP Level-4 Soil Moisture Product, *Journal of Hydrometeorology, 22*, 405-424, doi:10.1175/JHM-D-20-0217.1.

Rowlandson, T., S. Impera, J. Belanger, A. A. Berg, B. Toth, and R. Magagi (2015), Use of in situ soil moisture network for estimating regional-scale soil moisture during high soil moisture conditions, *Canadian Water Resources Journal / Revue canadienne des ressources hydriques, 40*, 343–351, doi:10.1080/07011784.2015.1061948.

Sanchez, N., J. Martinez-Fernandez, A. Scaini, and C. Perez-Gutierrez (2012), Validation of the SMOS L2 Soil Moisture Data in the REMEDHUS Network (Spain), *IEEE Transactions on Geoscience and Remote Sensing, 50*, 1602–1611, doi:10.1109/tgrs.2012.2186971.

Schaefer, G. L., M. H. Cosh, and T. J. Jackson (2007), The USDA Natural Resources Conservation Service Soil Climate Analysis Network (SCAN), *Journal of Atmospheric and Oceanic Technology, 24*, 2073–2077, doi:10.1175/2007jtecha930.1.

Seyfried, M. S., M. D. Murdock, C. L. Hanson, G. N. Flerchinger, and S. Van Vactor (2001), Long-Term Soil Water Content Database, Reynolds Creek Experimental Watershed, Idaho, United States, *Water Resources Research*, 37(11), 2847–2851, doi:10.1029/2001wr000419.

Simard, M., N. Pinto, J. B. Fisher, and A. Baccini (2011), Mapping forest canopy height globally with spaceborne lidar, *J. Geophys. Res., 116*, G04021, doi:10.1029/2011JG001708.

Smith, A. B., J. P. Walker, A. W. Western, R. I. Young, K. M. Ellett, R. C. Pipunic, R. B. Grayson, L. Siriwardena, F. H. S. Chiew, and H. Richter (2012), The Murrumbidgee soil moisture monitoring network data set, *Water Resources Research, 48*, doi:10.1029/2012wr011976.

Tan, J., G. J. Huffman, D. T. Bolvin, and E. J. Nelkin (2019), IMERG V06: Changes to the Morphing Algorithm. *Journal of Atmospheric and Oceanic Technology, 36*, 2471–2482, doi:10.1175/jtech-d-19-0114.1.

Tao, J., R. H. Reichle, R. D. Koster, B. A. Forman, and Y. Xue (2017), Evaluation and enhancement of permafrost modeling with the NASA Catchment Land Surface Model, *Journal of Advances in Modeling Earth Systems, 9*, 2771-2795, doi:10.1002/2017MS001019.

Tao, J., R. D. Koster, R. H. Reichle, B. A. Forman, Y. Xue, R. H. Chen, and M. Moghaddam (2019), Permafrost Variability over the Northern Hemisphere Based on the MERRA-2 Reanalysis, *The Cryosphere, 13*, 2087-2110, doi:10.5194/tc-13-2087-2019.

Tetlock, E., B. Toth, A. Berg, T. Rowlandson, and J. T. Ambadan (2019), An 11-year (2007–2017) soil moisture and precipitation dataset from the Kenaston Network in the Brightwater Creek basin, Saskatchewan, Canada, *Earth System Science Data, 11*, 787–796, doi:10.5194/essd-11-787-2019.

Thibeault, M., J. M. Caceres, D. Dadamia, A. G. Soldano, M. U. Quirno, J. M. Guerrieri, et al. (2015), Spatial and temporal analysis of the Monte Buey SAOCOM and SMAP core site. In 2015 IEEE International Geoscience and Remote Sensing Symposium (IGARSS), IEEE, doi:10.1109/igarss.2015.7325929.

Wagner, W., S. Hahn, R. Kidd, T. Melzer, Z. Bartalis, S. Hasenauer, et al. (2013), The ASCAT Soil Moisture Product: A Review of its Specifications, Validation Results, and Emerging Applications, *Meteorologische Zeitschrift, 22*, 5-33, doi:10.1127/0941-2948/2013/0399.

Wen, X., H. Lu, C. Li, T. Koike, and I, Kaihotsu. (2014), Inter-comparison of soil moisture products from SMOS, AMSR-E, ECWMF and GLDAS over the Mongolia Plateau. In T. J. Jackson, J. M. Chen, P. Gong, and S. Liang (Eds.), *Land Surface Remote Sensing II*, SPIE, doi: 10.1117/12.2068952.

Previous Volumes in This Series

Volume 1 September 1994	*Documentation of the Goddard Earth Observing System (GEOS) general circulation model - Version 1* L.L. Takacs, A. Molod, and T. Wang
Volume 2 October 1994	*Direct solution of the implicit formulation of fourth order horizontal diffusion for gridpoint models on the sphere* Y. Li, S. Moorthi, and J.R. Bates
Volume 3 December 1994	*An efficient thermal infrared radiation parameterization for use in general circulation models* M.-D. Chou and M.J. Suarez
Volume 4 January 1995	*Documentation of the Goddard Earth Observing System (GEOS) Data Assimilation System - Version 1* James Pfaendtner, Stephen Bloom, David Lamich, Michael Seablom, Meta Sienkiewicz, James Stobie, and Arlindo da Silva
Volume 5 April 1995	*Documentation of the Aries-GEOS dynamical core: Version 2* Max J. Suarez and Lawrence L. Takacs
Volume 6 April 1995	*A Multiyear Assimilation with the GEOS-1 System: Overview and Results* Siegfried Schubert, Chung-Kyu Park, Chung-Yu Wu, Wayne Higgins, Yelena Kondratyeva, Andrea Molod, Lawrence Takacs, Michael Seablom, and Richard Rood
Volume 7 September 1995	*Proceedings of the Workshop on the GEOS-1 Five-Year Assimilation* Siegfried D. Schubert and Richard B. Rood
Volume 8 March 1996	*Documentation of the Tangent Linear Model and Its Adjoint of the Adiabatic Version of the NASA GEOS-1 C-Grid GCM: Version 5.2* Weiyu Yang and I. Michael Navon
Volume 9 March 1996	*Energy and Water Balance Calculations in the Mosaic LSM* Randal D. Koster and Max J. Suarez

Volume 10 April 1996	*Dynamical Aspects of Climate Simulations Using the GEOS General Circulation Model* Lawrence L. Takacs and Max J. Suarez
Volume 11 May 1997	*Documentation of the Tangent Linear and Adjoint Models of the Relaxed Arakawa-Schubert Moisture Parameterization Package of the NASA GEOS-1 GCM (Version 5.2)* Weiyu Yang, I. Michael Navon, and Ricardo Todling
Volume 12 August 1997	*Comparison of Satellite Global Rainfall Algorithms* Alfred T.C. Chang and Long S. Chiu
Volume 13 December 1997	*Interannual Variability and Potential Predictability in Reanalysis Products* Wie Ming and Siegfried D. Schubert
Volume 14 August 1998	*A Comparison of GEOS Assimilated Data with FIFE Observations* Michael G. Bosilovich and Siegfried D. Schubert
Volume 15 June 1999	*A Solar Radiation Parameterization for Atmospheric Studies* Ming-Dah Chou and Max J. Suarez
Volume 16 November 1999	*Filtering Techniques on a Stretched Grid General Circulation Model* Lawrence Takacs, William Sawyer, Max J. Suarez, and Michael S. Fox-Rabinowitz
Volume 17 July 2000	*Atlas of Seasonal Means Simulated by the NSIPP-1 Atmospheric GCM* Julio T. Bacmeister, Philip J. Pegion, Siegfried D. Schubert, and Max J. Suarez
Volume 18 December 2000	*An Assessment of the Predictability of Northern Winter Seasonal Means with the NSIPP1 AGCM* Philip J. Pegion, Siegfried D. Schubert, and Max J. Suarez
Volume 19 July 2001	*A Thermal Infrared Radiation Parameterization for Atmospheric Studies* Ming-Dah Chou, Max J. Suarez, Xin-Zhong Liang, and Michael M.-H. Yan

Volume 20 August 2001	*The Climate of the FVCCM-3 Model* Yehui Chang, Siegfried D. Schubert, Shian-Jiann Lin, Sharon Nebuda, and Bo-Wen Shen
Volume 21 September 2001	*Design and Implementation of a Parallel Multivariate Ensemble Kalman Filter for the Poseidon Ocean General Circulation Model* Christian L. Keppenne and Michele M. Rienecker
Volume 22 August 2002	*A Coupled Ocean-Atmosphere Radiative Model for Global Ocean Biogeochemical Models* Watson W. Gregg
Volume 23 November 2002	*Prospects for Improved Forecasts of Weather and Short-term Climate Variability on Subseasonal (2-Week to 2-Month) Time Scales* Siegfried D. Schubert, Randall Dole, Huang van den Dool, Max J. Suarez, and Duane Waliser
Volume 24 July 2003	*Temperature Data Assimilation with Salinity Corrections: Validation for the NSIPP Ocean Data Assimilation System in the Tropical Pacific Ocean, 1993–1998* Alberto Troccoli, Michele M. Rienecker, Christian L. Keppenne, and Gregory C. Johnson
Volume 25 December 2003	*Modeling, Simulation, and Forecasting of Subseasonal Variability* Duane Waliser, Siegfried D. Schubert, Arun Kumar, Klaus Weickmann, and Randall Dole
Volume 26 April 2005	*Documentation and Validation of the Goddard Earth Observing System (GEOS) Data Assimilation System – Version 4* Senior Authors: S. Bloom, A. da Silva and D. Dee Contributing Authors: M. Bosilovich, J-D. Chern, S. Pawson, S. Schubert, M. Sienkiewicz, I. Stajner, W-W. Tan, and M-L. Wu
Volume 27 December 2008	*The GEOS-5 Data Assimilation System - Documentation of Versions 5.0.1, 5.1.0, and 5.2.0.* M.M. Rienecker, M.J. Suarez, R. Todling, J. Bacmeister, L. Takacs, H.-C. Liu, W. Gu, M. Sienkiewicz, R.D. Koster, R. Gelaro, I. Stajner, and J.E. Nielsen

Volume 28 April 2012	*The GEOS-5 Atmospheric General Circulation Model: Mean Climate and Development from MERRA to Fortuna* Andrea Molod, Lawrence Takacs, Max Suarez, Julio Bacmeister, In-Sun Song, and Andrew Eichmann
Volume 29 June 2012	*Atmospheric Reanalyses – Recent Progress and Prospects for the Future.* *A Report from a Technical Workshop, April 2010* Michele M. Rienecker, Dick Dee, Jack Woollen, Gilbert P. Compo, Kazutoshi Onogi, Ron Gelaro, Michael G. Bosilovich, Arlindo da Silva, Steven Pawson, Siegfried Schubert, Max Suarez, Dale Barker, Hirotaka Kamahori, Robert Kistler, and Suranjana Saha
Volume 30 December 2012	*The GEOS-iODAS: Description and Evaluation* Guillaume Vernieres, Michele M. Rienecker, Robin Kovach and Christian L. Keppenne
Volume 31 March 2013	*Global Surface Ocean Carbon Estimates in a Model Forced by MERRA* Watson W. Gregg, Nancy W. Casey and Cécile S. Rousseaux
Volume 32 March 2014	*Estimates of AOD Trends (2002-2012) over the World's Major Cities based on the MERRA Aerosol Reanalysis* Simon Provencal, Pavel Kishcha, Emily Elhacham, Arlindo M. da Silva, and Pinhas Alpert
Volume 33 August 2014	*The Effects of Chlorophyll Assimilation on Carbon Fluxes in a Global Biogeochemical Model* Cécile S. Rousseaux and Watson W. Gregg
Volume 34 September 2014	*Background Error Covariance Estimation using Information from a Single Model Trajectory with Application to Ocean Data Assimilation into the GEOS-5 Coupled Model* Christian L. Keppenne, Michele M. Rienecker, Robin M. Kovach, and Guillaume Vernieres
Volume 35 December 2014	*Observation-Corrected Precipitation Estimates in GEOS-5* Rolf H. Reichle and Qing Liu

Volume 36
March 2015

Evaluation of the 7-km GEOS-5 Nature Run

Ronald Gelaro, William M. Putman, Steven Pawson, Clara Draper, Andrea Molod, Peter M. Norris, Lesley Ott, Nikki Prive, Oreste Reale, Deepthi Achuthavarier, Michael Bosilovich, Virginie Buchard, Winston Chao, Lawrence Coy, Richard Cullather, Arlindo da Silva, Anton Darmenov, Ronald M. Errico, Marangelly Fuentes, Min-Jeong Kim, Randal Koster, Will McCarty, Jyothi Nattala, Gary Partyka, Siegfried Schubert, Guillaume Vernieres, Yuri Vikhliaev, and Krzysztof Wargan

Volume 37
March 2015

Maintaining Atmospheric Mass and Water Balance within Reanalysis

Lawrence L. Takacs, Max Suarez, and Ricardo Todling

Volume 38
September 2015

The Quick Fire Emissions Dataset (QFED) – Documentation of versions 2.1, 2.2 and 2.4

Anton S. Darmenov and Arlindo da Silva

Volume 39
September 2015

Land Boundary Conditions for the Goddard Earth Observing System Model Version 5 (GEOS-5) Climate Modeling System - Recent Updates and Data File Descriptions

Sarith Mahanama, Randal Koster, Gregory Walker, Lawrence Takacs, Rolf Reichle, Gabrielle De Lannoy, Qing Liu, Bin Zhao, and Max Suarez

Volume 40
October 2015

Soil Moisture Active Passive (SMAP) Project Assessment Report for the Beta-Release L4_SM Data Product

Rolf H. Reichle, Gabrielle J. M. De Lannoy, Qing Liu, Andreas Colliander, Austin Conaty, Thomas Jackson, John Kimball, and Randal D. Koster

Volume 41
October 2015

GDIS Workshop Report

Siegfried Schubert, Will Pozzi, Kingtse Mo, Eric Wood, Kerstin Stahl, Mike Hayes, Juergen Vogt, Sonia Seneviratne, Ron Stewart, Roger Pulwarty, and Robert Stefanski

Volume 42
November 2015

Soil Moisture Active Passive (SMAP) Project Calibration and Validation for the L4_C Beta-Release Data Product

John Kimball, Lucas Jones, Joseph Glassy, E. Natasha Stavros, Nima Madani, Rolf Reichle, Thomas Jackson, and Andreas Colliander

Volume 43
September 2015

MERRA-2: Initial Evaluation of the Climate

Michael G. Bosilovich, Santha Akella, Lawrence Coy, Richard Cullather, Clara Draper, Ronald Gelaro, Robin Kovach, Qing Liu, Andrea Molod,

Peter Norris, Krzysztof Wargan, Winston Chao, Rolf Reichle, Lawrence Takacs, Yury Vikhliaev, Steve Bloom, Allison Collow, Stacey Firth, Gordon Labow, Gary Partyka, Steven Pawson, Oreste Reale, Siegfried Schubert, and Max Suarez

Volume 44
February 2016

Estimation of the Ocean Skin Temperature using the NASA GEOS Atmospheric Data Assimilation System

Santha Akella, Ricardo Todling, Max Suarez

Volume 45
October 2016

The MERRA-2 Aerosol Assimilation

C. A. Randles, A. M. da Silva, V. Buchard, A. Darmenov, P. R. Colarco, V. Aquila, H. Bian, E. P. Nowottnick, X. Pan, A. Smirnov, H. Yu, and R. Govindaraju

Volume 46
October 2016

The MERRA-2 Input Observations: Summary and Assessment

Will McCarty, Lawrence Coy, Ronald Gelaro, Albert Huang, Dagmar Merkova, Edmond B. Smith, Meta Sienkiewicz, and Krzysztof Wargan

Volume 47
May 2017

An Evaluation of Teleconnections Over the United States in an Ensemble of AMIP Simulations with the MERRA-2 Configuration of the GEOS Atmospheric Model.

Allison B. Marquardt Collow, Sarith P. Mahanama, Michael G. Bosilovich, Randal D. Koster, and Siegfried D. Schubert

Volume 48
July 2017

Description of the GMAO OSSE for Weather Analysis Software Package: Version 3

Ronald M. Errico, Nikki C. Prive, David Carvalho, Meta Sienkiewicz, Amal El Akkraoui, Jing Guo, Ricardo Todling, Will McCarty, William M. Putman, Arlindo da Silva, Ronald Gelaro, and Isaac Moradi

Volume 49
March 2018

Preliminary Evaluation of Influence of Aerosols on the Simulation of Brightness Temperature in the NASA Goddard Earth Observing System Atmospheric Data Assimilation System

Jong Kim, Santha Akella, Will McCarty, Ricardo Todling, and Arlindo M. da Silva

Volume 50
March 2018

The GMAO Hybrid Ensemble-Variational Atmospheric Data Assimilation System: Version 2.0

Ricardo Todling and Amal El Akkraoui

Volume 51 July 2018	*The Atmosphere-Ocean Interface Layer of the NASA Goddard Earth Observing System Model and Data Assimilation System* Santha Akella and Max Suarez
Volume 52 July 2018	*Soil Moisture Active Passive (SMAP) Project Assessment Report for Version 4 of the L4_SM Data Product* Rolf H. Reichle, Qing Liu, Randal D. Koster, Joe Ardizzone, Andreas Colliander, Wade Crow, Gabrielle J. M. De Lannoy, and John Kimball
Volume 53 October 2019	*Ensemble Generation Strategies Employed in the GMAO GEOS-S2S Forecast System* Siegfried Schubert, Anna Borovikov, Young-Kwon Lim, and Andrea Molod
Volume 54 August 2020	*Position Estimation of Atmospheric Motion Vectors for Observation System Simulation Experiments* David Carvalho and Will McCarty
Volume 55 February 2021	*A Phenomenon-Based Decomposition of Model-Based Estimates of Boreal Winter ENSO Variability* Siegfried Schubert, Young-Kwon Lim, Andrea Molod, and Allison Collow
Volume 56 June 2021	*Validation Assessment for the Soil Moisture Active Passive (SMAP) Level 4 Carbon (L4_C) Data Product Version 5* John S. Kimball, K. Arthur Endsley, Tobias Kundig, Joseph Glassy, Rolf H. Reichle, and Joseph V. Ardizzone
Volume 57 July 2021	*Tendency Bias Correction in the GEOS AGCM* Yehui Chang, Siegfried Schubert, Randal Koster, and Andrea Molod